



Università degli Studi di Milano

GRADUATE SCHOOL OF VETERINARY SCIENCES FOR ANIMAL
HEALTH AND FOOD SAFETY

Director: Prof. Valentino Bontempo

Doctoral Program in Veterinary Clinical Sciences

XXVIII CYCLE

Academic Year: 2014-2015

STRAIN ELASTOGRAPHY IN DOGS: APPROACH TO SOME CLINICAL APPLICATIONS

Dr. Gabriele Barella

R09966

Tutor: Prof. Stefano Faverzani

Coordinator: Prof. Fausto Cremonesi

CHAPTER 1 - Introduction

1. Introduction p.5

CHAPTER 2 - Aim of the study

2. Aim of the study p.8

CHAPTER 3 - Elastasonography: bases, techniques and pitfalls

3.1 Elastasonography: bases, techniques and pitfalls p.10

3.2 Bases p.10

3.3 Elastasonographic techniques p.14

3.4 Performing modalities of Strain Elastasonography p.15

3.5 Strain Elastasonography: measurements p.17

3.6 Pitfalls p.19

CHAPTER 4 - Elastasonography: reports in veterinary medicine

4. Elastasonography: reports in veterinary medicine p.22

CHAPTER 5 - Application of strain elastography in the evaluation of hypoechoic splenic lesions in dogs

5.1 Introduction p.25

5.2 Materials and methods p.26

5.3 Results p.28

5.4 Discussion p.32

CHAPTER 6 - Application of strain elastography in the evaluation of mammary lesions in dogs

6.1 Introduction p.36

6.2 Materials and methods p.37

6.3 Results p.39

6.4 Discussion p.43

CHAPTER 7 - Application of strain elastography in the evaluation of superficial lesions in dogs: comparing two score systems

7.1 Introduction p.52

7.2 Materials and methods p.53

7.3 Results p.55

7.4 Discussion p.74

CHAPTER 8 - Conclusions

8. Conclusions p.79

CHAPTER 9 - References

9. References p.81

CHAPTER 1

INTRODUCTION

1. Introduction

Pathological changes in biological tissues are associated to different tissue stiffness and elasticity (Shiina, 2014). The possibility to access tissue elasticity and its distribution may have many important clinical applications. It can be used for the early diagnosis of those pathologies that affect tissues properties when morphological changes have been not observed yet. On the basis of tissue elasticity it may be possible to define the degree of progression of a disease (such as a tumor) evaluating its extent. Finally the response to a treatment can be evaluated considering that often the stiffness of a lesion changes as a result of therapies (i.e. chemotherapy or radiofrequency ablation) (Shiina,2014). Palpation is an essential component in clinical evaluation and represents the ancient method for the assessment of tissue characteristics. However its application is limited to accessible organs and the interpretation of the informations obtained is subjective. Real-time or strain elastography (SE) is a not invasive ultrasonographic technique that

can be used in medicine to assess tissue characteristics (stiffness) evaluating tissue displacement in response to an applied force. The deforming force applied to the tissue derives from an external compressor (e.g. perpendicular movements of the ultrasound transducer) or from physiologic functions (e.g. breathing, cardiac movements) (White, 2013). The usefulness of this method is based on the fact that pathological changes in tissues also affects in their stiffness (neoplasia tends to be harder than normal tissue due to high cell density). Differences in tissue displacement (called strain) are calculated and presented as a color map (elastogram) that overlaps the B-mode image. The color map documents the relative elasticity of the tissues included in the region of interest expressed in different colors. The deformability of the organ

(elasticity) depends on the tissue composition; neoplastic tissues have higher cell density and therefore a reduced elasticity (increased tissue stiffness) (Goddi, 2012). Similarly fluids, physically, can not be compressed and an increase blood flow in an organ increases its hardness (Hirooka, 2011). In human medicine malignant parenchymal lesions are significantly stiffer than surrounding normal parenchyma (Barr, 2012; Teng, 2012; Wang 2013; Wells, 2011). In the last five years academic societies of medical ultrasound such as the World Federation for Ultrasound in Medicine and Biology (WFUMB), the European federation of Societies for Ultrasound in Medicine and Biology (EFSUMB) and the Japan Society of Ultrasonics in Medicine (JSUM) proposed guidelines for the clinical use of elastography in human medicine (Bamber, 2013; Barr, 2015; Cosgrove, 2013). Recently this technique have started to be available also in small animal practice attracting the interest of clinicians.

CHAPTER 2

AIM OF THE STUDY

2. Aim of the study

Currently in veterinary medicine the publications concerning the application of SE and its usefulness in the small animal practice are a few. The purpose of this study is to evaluate the applicability and the clinical utility of this new ultrasonographic technique in the study of splenic lesions, mammary tumors and skin lesions in dogs trying to assess whether the different methods of data evaluation (qualitative and quantitative) proposed in human medicine can be applied to canine patients.

CHAPTER 3

ELASTOSONOGRAPHY: BASES, TECHNIQUES AND PITFALLS

3.1 Elastasonography: bases, techniques and pitfalls

Elastasonography is a modern technique that has been developed in human medicine since the early nineties, which aims to assess the degree of tissue elasticity (Ophir, 1999). The first publications regarding the presence of shear waves and surface waves in the soft tissue date back to 1950. In these studies it is evident that the propagation of these waves depend on the viscoelasticity of the medium in which they are contained (Sarvazyan, 2011) . Kit Hill in 1976, has tried to develop an ultrasonographic method to analyze the movements of tissues: he developed the idea that from the movements of tissues it is possible to obtain much information about the mechanical properties of the different materials that make up a body (Sarvazyan, 2011). In 1980, some studies have highlighted the possibility to use ultrasound through a real-time technique to evaluate the deformability of tissues when subjected to a pressure (Wojcinski, 2012). With this new method Ophir et al. in 1999 could assess the difference in elasticity between some tissues affected by pathological forms of different nature compared to healthy ones (Sarvazyan, 2011). The first studies carried out mainly on the mammary gland and on the prostate gland have shown, in fact, a substantial difference in terms of rigidity regarding benign and malignant lesions and described how a greater rigidity is correlated, more frequently, to the presence of malignant lesions (Ophir, 1999). This was also confirmed by subsequent studies carried out on different organs, such as mammary gland, prostate gland, lymph nodes, liver and thyroid, thus highlighting the usefulness of this new diagnostic method to differentiate benign from malignant diseases (Lyshchik, 2005; Itoh, 2006; Alam, 2008; Asteria, 2008; Bhatia, 2010).

3.2 Bases

The elastic deformation is the fundamental principle on which elastography is based on. This is a mechanical feature that explains why a body, subjected to a pressure, is deformed in a variable way depending on both the intensity of the applied force and the inherent characteristics of the body. The deformation, in fact, is different in different tissues (fat, collagen, muscle), but also within the same tissue when penetrated by pathological states (inflammations, tumors) (Alam, 2008). This can be explained considering that the elastic properties of a tissue essentially depend on the molecular structure of the tissue itself, and then, following an alteration of this structure, it will also have a change of the elastic deformation (Ophir, 1999).

Elastography uses two basic concepts:

- There are significant differences in the mechanical properties of the different tissue components;
- In many diseases the tissue elasticity changes quite significantly.

Thus pathological alterations determine variations of hardness of the tissues in which they are present: many tumors can be hard, benign lesions may be harder than the surrounding tissues but softer than malignant lesions (Arda, 2011). On the same principle it is based palpation, a diagnostic technique used since ancient times and considered an excellent screening tool that allows to consider the possible diagnosis for the evaluated abnormalities. However, this technique presents limits because it allows to evaluate only superficial and directly accessible organs, and also both the execution and the interpretation are strongly subjective. With the introduction of the elastographic techniques it was possible to overcome these obstacles (Bamber, 2013). In elastography a mechanical force (compression or vibration) is applied to a tissue and some diagnostic imaging techniques (such as ultrasound and magnetic resonance

imaging) are used to create a map of tissue deformation (Nazarian, 2007). In elastosonography the representation of the hardness of the tissue can be obtained using a traditional ultrasound machine with a special software (Alam, 2008). Elastosonography found increasingly spread in human medicine as it has increased significantly the diagnostic power of ultrasound (Wojcinski, 2012). The traditional B-mode ultrasound generates an image by reflection and scattering of ultrasound for different acoustic impedance of tissues. Elastosonography, however, allows the assessment of tissue elasticity highlighting, in a chromatic scale, the modification of the tissue deformation (Bamber, 2013). The elasticity of a tissue is estimated considering the deformation that the surrounding tissues refer when a compressive force is applied (Figure 1). The resulting image is called elastogram and it is processed in several steps: first, the machine receives the digitized radiofrequency echo-lines from the tissue, which is then subjected to a series of compressions determinants some deformation depending on the type of tissue and finally receives again some radiofrequency echo-lines from the same tissue. The collected data resulting from these two echo-lines are processed and they make up the image (elastogram) on the screen (Alam, 2008). There are two types of elastograms (Figure 2): a grayscale in which hard tissue appears as black and soft tissues as light-gray; a color scale in which the increase in hardness of a tissue appears in ascending order as red, yellow, green and blue (Alam, 2008). However the color scheme showing the hard and soft area can be changed according to the operators choice.

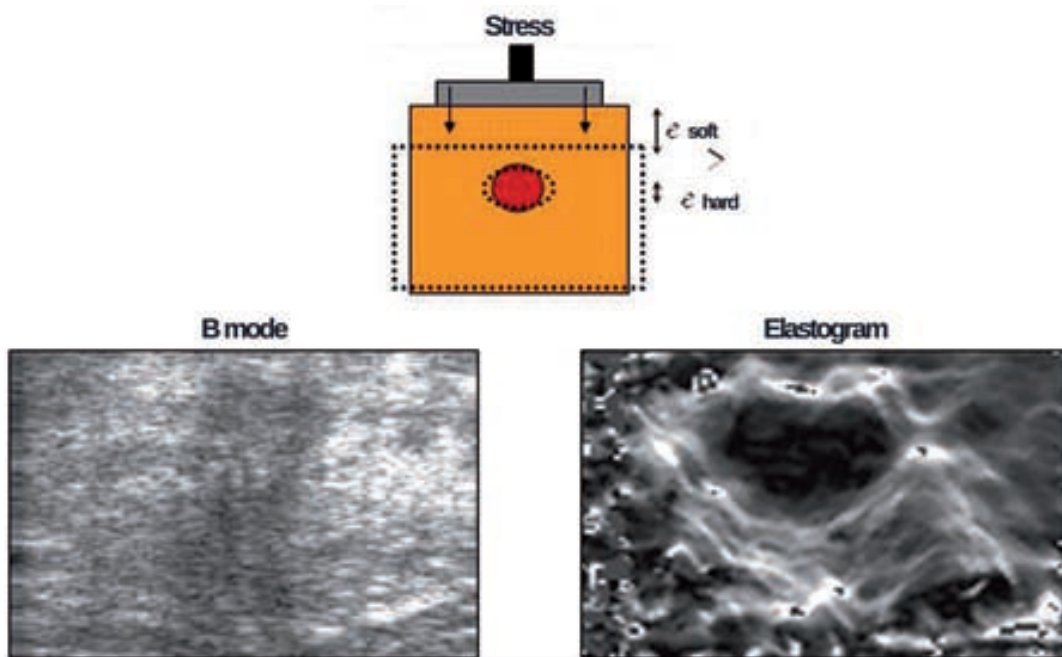


Figure 1: Scheme of a compressive force applied to a body and comparison between a B-mode image and an elastosonographic image.

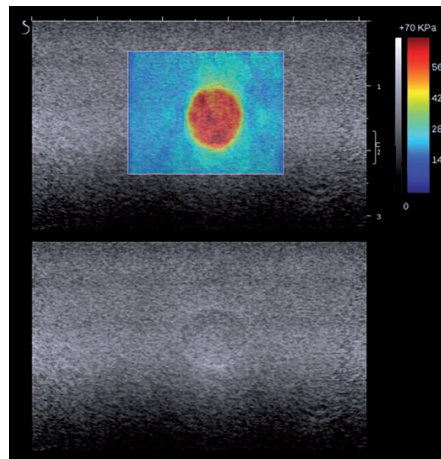


Figure 2: Color and grayscale elastograms.

The mechanical modifications induced by palpation or by elastography create forces, in the tissue, acting against this type of deformation, which are called shear. There are two types of shear: the "simple shear" (the result of a compressive force that is applied in a single point of the object that determines a change of its shape, without however having an alteration in volume of the same) and the "pure shear" (the result of a vertical compressive

force that is applied to move the entire surface of the body and which determines a compression in the vertical direction and an expansion in the horizontal direction of the body, without determining, alterations of its volume. The simple shear are produced by acoustic radiation, while the pure shear from the ultrasound transducer (Bamber, 2013). The elasticity of a material describes its tendency to return back to the original size and shape after being subjected to a deforming force, which is called stress. Using elastosonography the stress is performed with the compression of the ultrasound probe on the tissue. The deformation that follows, instead, is called strain (Wells, 2011). The relationship between stress and strain is a constant called the modulus of elasticity which is a measure for the physical deformability of a body, expressed in units of Pascal pressure or kiloPascals (Arda, 2011).

3.3 Elastosonographic techniques

Depending on the force applied to the organ or tissue we can classify elastosonography as static/semi-static (when the tissue is subjected to a constant stress and its deformation may be measured) or dynamic when the tissue is subjected to a transient or oscillatory mechanical force at a fixed frequency (Bamber, 2013; Greenleaf, 2003). The *Static Elastosonography* is a qualitative analysis. Considering that the tissues are stressed by the pressure produced by the ultrasound probe, and there is no information regarding the force exerted on the tissue, it is not possible to calculate the absolute stiffness of the tissue examined. The deformation produced is calculated in relation to the surrounding tissue. This is a relative analysis due to deformation observed is strictly dependent on the tissue included in the area of interest. The *Strain Elastography* (SE or real time elastography) and the *Acoustic Radiation Force*

Impulse Imaging (ARFI) are two types of static elastographic techniques. The SE was the first technique available on traditional ultrasound devices as it can be performed with the only introduction of a new software. It measures the "strain" or deformability of a tissue undergoing an uniform longitudinal compression. Compression can be applied by the operator through the transducer or taking advantage of some physiological movements such as the pulsing of vessels, the breathing movements or muscle vibration. The data on the strain of the tissue analyzed are then represented on a map in two dimensions and color scale, called elastogram. The limit of this technique is to be able to evaluate only the strain, while no information is provided about the magnitude and the distribution of stress. (Greenleaf, 2003). The ARFI technique is based on the acoustic radiation force generated directly on a target point in the tissue analyzed. The acoustic radiation force impulse produces shear waves in the tissue, which are then picked up by the probe itself. The technique has the advantage that the stress is applied from the probe directly onto the tissue of interest and this avoids the interference with surrounding organs (Greenleaf, 2003). Some quantitative parameters can be calculated such as: the speed of the shear waves (which is directly proportional to the hardness of the tissue examined), the time to reach the maximum deformation, the magnitude of this deformation, the time taken to return to the original position and shape (Monpeyssen, 2013). The *Dynamic Elastosonography*, instead, allows the measurements of the shear waves generated in a tissue undergoing mechanical deformation. Ideally the propagation speed of the waves is determined solely by the density of the organ. The ultrasound in this method is used to record the propagation of shear waves that reflects the viscoelasticity of tissues (Bamber, 2013). The stress applied originates from sources external or internal to the body. The informations obtained by the dynamic elastosonography are expressed in

measurements using the *Transient Elastasonography* and the *Point Shear Wave Elastasonography* or in imaging using the *Shear Wave Elastasonography* (Greenleaf, 2003). The *Transient Elastasonography* uses an external vibrator to produce tissue deformations and it uses an ultrasonographic probe in order to record the propagation of the elastic wave. The *Shear Wave Elastasonography* is based on the acoustic radiation applied to a tissue in vertical direction determines in it horizontal shear waves. The speed of these waves can be measured in kiloPascal. This value expresses the stiffness of the tissue or organ at a particular point of interest. The higher the value in kiloPascals is, greater is the stiffness of the lesion evaluated. This corresponds to a greater likelihood that the lesion is malignant (Monpeyssen, 2013). Compared to other methods, this has the advantage to allow a semiquantitative measurement; it is operator independent because it does not require movement of the probe and it can be therefore easily reproducible (Arda, 2011; Wojcinski, 2012; Monpeyssen, 2013). The *Point Shear Wave Elastasonography* measures the time the shear waves take to cross the organ analyzed. The obtained data provide an average speed value of the shear waves that is proportional to the degree of stiffness of the tissue.

3.4 Performing modalities of Strain Elastasonography

Stain Elastography is performed through compression and retraction movements of the probe on the tissue. It is very important that the probe, during the movements, is positioned as perpendicular as possible to the scanning surface. A region of interest (ROI) on the b-mode image must be selected. The ROI must be four times the size of the lesion to assess because it is important that there is an adequate amount of normal tissue in order to evaluate the difference in hardness. The lesion of interest must be placed in the center of the ROI (Dudea, 2013). An alternating series of pressures and

retractions of the probe with rhythmic movements must be performed as perpendicular as possible to the area analyzed. The elastosonographic image is not displayed if the movements are not correct, in order to guarantee the highest level of reliability. A graphical indicator, constituted by a series of spirals, provides information on the quality of the acquisition linked to the pressure movement performed. The spiral set is a progressive index: the first three spiral are gray and appear when the image is scanned correctly, the other three are green and appear only when the acquisition is correct. The more the spirals are represented more appropriate quality of movement and consequent more reliable the values are (Figure 4)._When the elastogram appears it is possible to evaluate the presence of soft and hard areas represented by different colors: some machines, especially the first to be marketed, represent hard areas in blue, while soft areas in red, while other machines use these colors in the opposite way (Dudea, 2013). In Figure 5 hard areas are coded in red while soft areas in green.

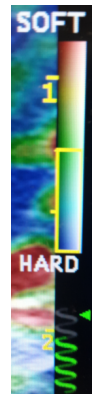


Figure 4: Graphic indicator consistent in a series of spirals that assume a green color when the image is scanned properly.

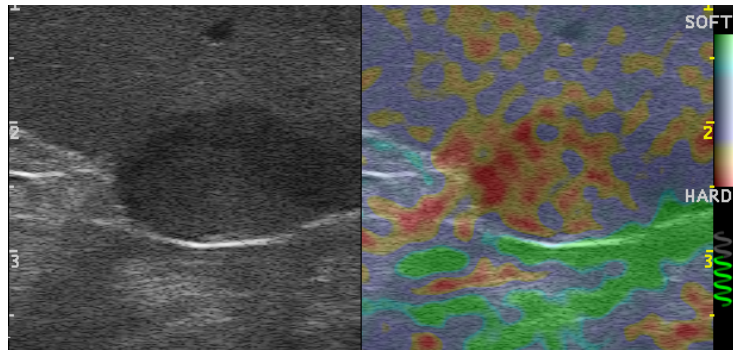


Figure 5: elastogram coding hard tissue in red and soft tissue in green.

3.5 Strain Elastosonography: measurements

Strain Ratio: is obtained by tracing on the elastosonographic image two zones of the same size ($z1$ and $z2$) positioned in a tissue at the same depth (Figure 6). The system calculates the ratio between the deformability of the tissue included in the zone 2 compared to the deformability of the tissue included in zone 1. After this, it is possible to build a histogram that shows the distribution of different areas on the basis of a scale from 0 to 100 (Dudea, 2013, Monpeyssen, 2013).

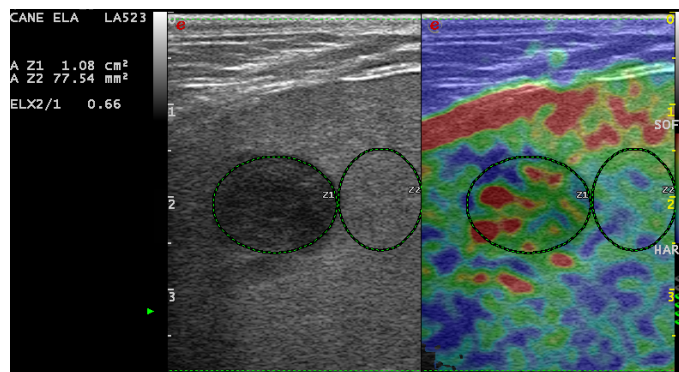


Figura 6: Strain ratio between $z1$ (the area corresponding to a splenic focal lesion) and $z2$ (corresponding to a portion of normal splenic parenchyma). The areas with high deformability are represented in red, those with medium deformability in green and those with a low deformability in blue.

Hardness Value: that counts the number of points (included in a traced area) which have a lower hardness than a defined threshold (Figure 7). The result of this count is expressed as a percentage.

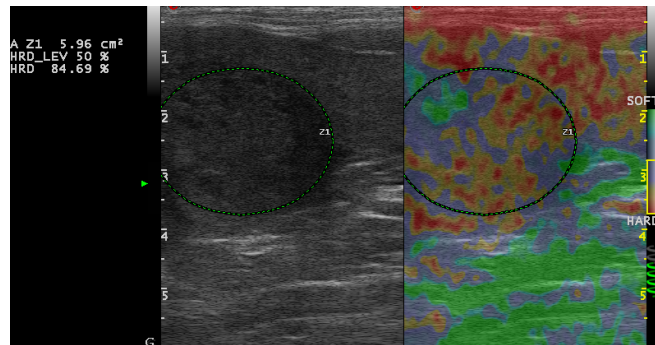


Figure 7: Hardness value of a focal splenic lesions. The areas with high deformability are represented in green while those with a low deformability in red.

Elastosonographic scores have been proposed in human medicine to distinguish the benign or malignant nature of lesions in different tissues. However, there is not an universally recognized method of interpretation and there are many classification systems (Bhatia, 2013). Some examples of classification score systems for lymph-nodes evaluations are listed below (Figure 8-9) (Dudea, 2013).

Table II. Classification of SE appearance of lymph nodes according to Alam [7].

Pattern				
1	2	3	4	5
Absent or very small hard area	Hard area < 45% of lymph node	Hard area > 45% of lymph node	Peripheral hard and central soft area	Hard area over the entire node, with or without soft rim

Table III. Classification of SE appearance of lymph nodes proposed by Furukawa [19,20]

Pattern			
1	2	3	4
> 80% of the cross sectional area is soft (red or green)	50 – 80% of the node area is soft (green or red)	50 – 80 % of the area is blue	> 80% of the node area is blue

Figure 8: Score systems from Dudea, 2013.

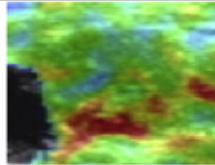
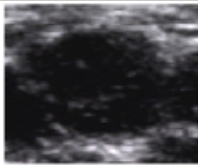
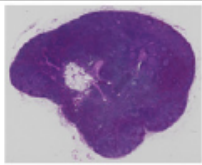
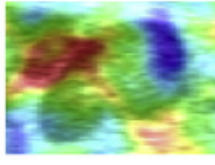
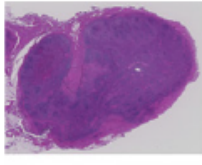
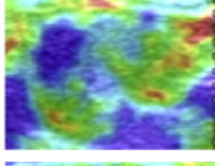
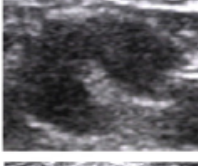
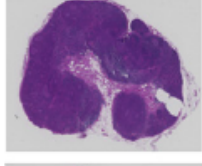
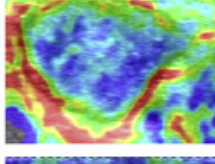
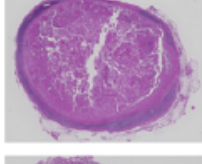
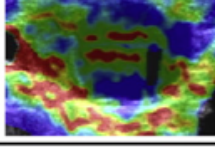
Score	Description			
1	No blue area			
2	Small blue area			
3	Half of LN colored blue			
4	More than half of the LN colored blue			
5	Peripheral blue area and central red, yellow or green area			

Figure 9: Score systems from Real-time tissue elastography for the diagnosis of lymph node metastasis in oral squamous cell carcinoma (Ishibashi , 2012).

3.6 Pitfalls

Although the ultrasonographic technique is simple and quick to learn, there are several factors related to the executions modalities and to the lesions characteristics that can affect the image (Ciurea, 2008). Artifacts may be either mechanical or acoustic (Ophir, 1999). The mechanical artifacts are related to the amount of the stress, or to the amplitude and the type of movement on the tissue. When an initial excessive pressure is applied on the tissue this causes a decrease in its normal elasticity, with a false negative result. This happens because during an initial compression, the relationship between strain and pressure is not linear. Another factor that influences the

image is compression with lateral movements or out of the image plane. The problems related to the execution mode can now be overcome thanks to some software systems for image quality evaluation. The acoustic artifact depends on the ultrasound technique. The presence of artifacts such as reverberations, deviation of the waves, posterior acoustic shadowing may imply misinterpretation. For this reason, elastography cannot be applied to calcified or cystic lesions. In fact, liquids dissipate the stress applied without sharing it to the solid surrounding tissues (Bhatia, 2013). The artifacts related to the lesions characteristics occur when the lesion to be analyzed is voluminous and occupies the entire region of interest (ROI). This prevents a comparison with the surrounding healthy tissue and, consequently, makes it difficult to interpret the image correctly. The lesion depth also affects interpretation. Elastography is not applicable if the lesion is located at a depth that exceeds the penetration capacity of the probe (almost 4 cm). Finally if neighboring structures have a stiffness very different among themselves the signal can be distorted: the soft tissues are deformed mostly when they are adjacent to very hard tissues (effect known as "Maltese cross"). Conversely a soft lesion surrounded by a stiff area is difficult to assess because the background acts as a hard shell that prevents the generation of strain within the lesion evaluated (effect known as "Eggshell") (Bhatia, 2013).

CHAPTER 4

ELASTOSONOGRAPHY: REPORTS IN VETERINARY MEDICINE

4. Elastasonography: reports in veterinary medicine

A few reports in veterinary medicine concern the study and the application of elastasonography in animal clinic. The Transient Elastography was used in a study in 2012 in order to evaluate the stiffness of hepatic tissue in dogs (Juarez, 2012) demonstrating its reproducibility. In 2013 a study conducted on horses used the Strain Elastography to assess tendons elasticity (Lustgarten, 2014), demonstrating repeatability and reproducibility. The study of White et al. in 2013 investigated the use the Strain Elastography in the evaluation of certain organs (liver, kidneys and spleen) in healthy cats. The aim of this study was to assess whether this new technique could be easily applied and could describe the normal elastasonographic appearance of liver, kidneys and spleen of healthy cats compared to the abdominal wall. The strain elastasonography was applied successfully and the authors proposed some practical tips for the proper execution and interpretation of the elastasonographic examination. The ARFI was used to study the elastasonographic characteristics of canine hepatic, splenic and renal parenchyma. In this study differences in tissue hardness depended on tissue depth (the speed of the shear waves decreases as the depth of the organ examined increases due to parenchymal attenuation) and patient weight (in obese patients the shear waves are significantly attenuated). (Holdsworth, 2013). Glinska-Suchocka et al. (2013) analyzed 12 breast tumors in dogs using the Shear wave elastography providing a method to difference benign lesions (significantly softer) from malignant lesions (significantly harder). The greater hardness of the malignant lesions can be caused by an abnormal benign stromal fibrous tissue (desmoplasia) occurring in most of these tumors. The authors pointed out that the results from this study have proven to be in perfect agreement with many works conducted in human medicine

regarding breast cancer. In 2014 Feliciano et al. used the ARFI for the study of mammary tumors in 50 dogs. In this study, the elastosonography added to the ultrasound evaluation a significant increment of the sensitivity in differentiate malignant lesions from benign lesions. The same author has performed the first study on the evaluation of the prostate and testicles through the ARFI technology in dogs obtaining mean values of elasticity that would be used in future studies aiming to differentiate malignant from benign lesions (Feliciano, 2015). They also evaluated, in another study, the application of the ARFI on the splenic parenchyma of healthy cats confirming its reproducibility, repeatability, and recording mean values of elasticity (Feliciano, 2015). The feasibility of Strain Elastography have been confirmed in 2015 by Jeon et al. This study estimated tissue stiffness in the canine liver, spleen, kidneys, and prostate providing basic information for strain values and strain ratios in clinically normal patients. In conclusion in 2015 Lee et al used the Strain Elastography for estimating thyroid stiffness in dogs. They demonstrated its feasibility taking advantage of the carotid artery pulsation induced by dobutamine infusion with excellent repeatability.

CHAPTER 5

APPLICATION OF STRAIN ELASTOGRAPHY IN THE EVALUATION OF HYPOECHOIC SPLENIC LESIONS IN DOGS

5. Application of Strain Elastography in the evaluation of hypoechoic splenic lesions in dogs

5.1 Introduction

Focal splenic lesions are alteration of the parenchyma that make the organ inhomogeneous and can cause a deformation of its profile. Splenic lesions are easily detected with ultrasound in dogs regardless of their clinical condition. Usually for big lesions or lesions with an high risk of rupture an elective splenectomy is strongly suggested, while small lesions still remain a diagnostic challenge. To our knowledge hyperechoic lesions are mostly benign while the not-hyperechoic lesions can be benign or malignant. Unfortunately the B-mode appearance of splenic lesions is not related to a specific disease. Even the color and power Doppler evaluation of blood flow to the spleen masses does not provide a reliable differentiation between benignity and malignancy (Sharpley, 2012). Moreover the contrast enhanced ultrasound has been defined as a limited screening diagnostic method and its role is questionable for splenic pathology (Ivancic, 2009; Ohlerth, 2008; Taeymans, 2011). Only the presence of tortuous feeding vessels, throughout all perfusion phases, may improve the accuracy in characterizing benign splenic lesions versus malignant (Taeymans, 2011). The fine needle aspiration can be considered as the first step towards an accurate diagnosis representing a low risk procedure that can be performed without sedation. This technique present an high sensibility for the diagnosis of extramedullary hematopoiesis or round cells neoplasia but is less sensible for connective tissue tumors that tends to exfoliate cells poorly (Hayes, 2012). However in some cases the location or the appearance (high risk of rupture) of the lesions makes it very

difficult if not impossible the ultrasound-guided percutaneous sampling. Sedation or general anesthesia for uncooperative patients are often required (Holdsworth, 2014); however this procedure can be not viable in case of critical patients. Needle core biopsy has been proposed a complementary method but the requirement of sedation, the costs and the possibility of major complications made the recurrence of this procedure questionable (Taeymans, 2011). Real-time or strain elastography is a not invasive technique that can be used in medicine to assess tissue stiffness or tissue displacement in response to an applied force. The deforming force applied to the tissue derives from an external compressor (e.g. perpendicular movements of the ultrasound transducer) or physiologic functions (e.g. breathing, cardiac movements) (White, 2013). The usefulness of this method is based on the fact that pathological changes in tissues also affects in their stiffness (neoplasia tends to be harder than normal tissue due to high cell density). Differences in tissue displacement (called strain) are calculated and presented as a color map (elastogram) that overlaps the B-mode image. The color map documents the relative elasticity of the tissues included in the region of interest expressed in different colors. The deformability of the organ (elasticity) depends on the tissue composition; neoplastic tissues have higher cell density and therefore a reduced elasticity (increased tissue stiffness) (Goddi, 2012). Similarly fluids, physically, can not be compressed and an increase blood flow in an organ increases its hardness (Hirooka, 2011). In human medicine malignant parenchymal lesions are significantly stiffer than surrounding normal parenchyma (Barr, 2012; Teng, 2012; Wang 2013; Wells, 2011). To our knowledge there are no studies concerning the evaluation of splenic lesions using real time elastosonography neither in humans or in small animal medicine. The aim of this study is to assess the repeatability and reproducibility of real time elastography in the evaluation of splenic lesions in

dogs and to verify if this technique can differentiate benign from malignant lesions.

5.2 Materials and Methods

Medical records belonging to dogs referred to our hospital, between January 2014 and January 2015, were evaluated in order to select all patients presented for abdominal ultrasound having a solitary hypoechoic splenic lesion as the only significant finding. All the ultrasonographic examinations were performed using an esaote MyLab 70 (Genova, Italy) equipped with a multifrequency linear transducer (7,5-13 MHz) in association with a Real-time Elastography module. Dogs were evaluated, after hair clipping and ultrasonographic gel applied, in right lateral recumbency in order to have the left part of the abdomen upward. Dogs underwent B-mode evaluation of the entire abdomen and elastosonographic evaluation of the spleen. The left intercostal approach was used to evaluate in longitudinal section the head of the spleen; the splenic body and tail were scanned throughout sagittal and transverse planes from the ventral and lateral abdominal wall. Each focal splenic lesion recorded in B-mode was measured in both diameters and only lesions of a maximum 4 cm width were selected. Only splenic lesions located at a maximum depth of 4 cm and not close to the visceral margins of the spleen were considered. Strain Elastography was used to assess the qualitative and relative stiffness of splenic lesions that were comprised in a selected region of interest (ROI). The selected ROI comprised all the sonographic field of view (a maximum of 5 cm depth) and included the entire splenic lesion and a same sized portion of normal splenic parenchyma almost located at the same depth. Stomach and great abdominal vessels were not considered in the ROI. The Real-time elastosonographic examination was performed in

succession by 2 operators maintaining the same parameters such as: acoustic window, depth, ROI size, gains and frequency. Tissue compression was performed, in order to obtain the elastogram of each lesion, using the ultrasonographic probe. The adequate amount of pressure was indicated by a grey spiral located on the screen that turned into green. Images were acquired after at least 5 seconds lingering of the green spiral. In the elastogram hard areas (areas of low strain) were coded in blue, intermediate stiffness areas were coded in green and soft areas were coded in red (areas of high strain). Each operator obtained 5 images of each splenic lesion and on this images 2 measurements were performed. The Strain Ratio (SR or rather z_2/z_1 ; where z_1 represented the entire lesion and z_2 represented a same size portion of normal splenic parenchyma located at the same depth) and the hardness value (HV; percentage of areas in the lesion coded as hard) were calculated for each lesion. The mean and standard deviations of all measurements performed by the two operators were calculated. All splenic lesions were subjected to ultrasound guided fine needle biopsy (“not aspiration” technique using a 22-23 Gauges needle) and/or histologic evaluation (performed after splenectomy). The Coefficient of Variability (CV) and the K of Cohen were calculated in order to assess the inter-observer and the intra-observer variability of this method respectively. The ANOVA and the Fisher exact test were used to verify the differences between the SR values and HV of benign versus malignant lesions. The cut-off value for the Fisher test was arbitrarily set at 1.5 for SR and at 70% for the HV. The Odds Ratio (OR) was also calculated considering: malignancy as bad outcome and dogs with values of HV >70% and SR > 1.5 in the exposed group. The sensibility (Se), the specificity (Sp), the positive predictive value (PPV), the negative predicting value (NPV), the positive likelihood ratio (PLR) and the negative likelihood ratio (NLR) were also calculated. A $p < 0.05$ was considered significant.

5.3 Results

Twenty-four dogs met the inclusion criteria: 2 Beagle, 1 Border Collie, 1 Boston Terrier, 5 English Cocker Spaniel, 1 English Foxhound, 1 Flat Coated retriever, 1 French Bulldog, 2 German Sheperd, 1 Golden Retriever, 1 Hovawart, 1 Italian Spinone, 2 Labrador Retriever, 4 Mixed Breed, 1 Shitzu. The mean age of patients was 10.430 ± 3.2 years old; 11 dogs were males (3 neutered) while 13 were females (12 neutered). Mean values of minor and major diameters of lesions were respectively; 1.35 ± 0.94 cm and $1.63 \pm 0,96$ cm. The biggest lesion measured 3.6 x 3.9 cm while the smallest 0.49 x 0.5 cm. Sixteen of 24 splenic lesions were benign (67%; 2 extramedullary hematopoiesis, 14 nodular hyperplasia) while 8 of 24 were malignant (33%; 6 hemangiosarcoma, 2 lymphoma). All dogs underwent fine needle biopsy followed in 6 cases by histology after splenectomy. The benignity of lesions was also confirmed in seven dogs presenting nodular hyperplasia followed and re-evaluated (B-mode and real time elastography) from 3 to 17 months after the first ultrasonographic exam. None of these patients presented any changes concerning the b-mode (dimension and echo-texture) and elastosonographic (SR and HV) appearance of splenic nodules. All these patients underwent a second fine needle biopsy of the lesion that showed the same diagnosis. No differences were observed between benign and malignant lesions considering: lesions size, canine sex and age ($p > 0.05$). Considering the SR significant differences were observed between benign (mostly soft) and malignant (mostly hard) lesions ($p < 0.05$). Choosing an arbitrary value of 1.5 statistically significant differences were observed between benign and malignant lesions ($p = 0.0003$; Se 75%, Sp 100%, PLR 0, NLR 0.25, PPV 100%, NPV 88.24%): no benign lesions presented a SR value ≥ 1.5 while 6 malignant lesions presented a SR value ≥ 1.5 and 2 malignant lesions < 1.5 .

(Table 1). In one case, due to poor image quality, the SR could not be calculated. Considering the HR significant differences were observed between benign (mostly soft) and malignant (mostly hard) lesions ($p < 0.05$). Choosing an arbitrary value of 70% statistically significant differences were observed between benign and malignant lesions ($p = 0.001$; Se 100%, Sp 75%, PLR 4, NLR 0, PPV 66,67%, NPV 100%): no malignant lesions presented a HV value $< 70\%$ while 12 benign lesions presented a HV $< 70\%$ and 4 benign lesions $\geq 70\%$ (Table 2). Data concerning single values of Strain ratios and hardness value are reported in Table 3. The CV values were 0.08 ± 0.03 for the SR and 0.08 ± 0.05 for the HV. The K of Cohen showed a perfect agreement between operators concerning the HV ($k = 1$) and a good agreement concerning the SR ($k = 0.66$). The OR showed that the correlation between SR ≥ 1.5 and malignancy was statistically significant (OR, 80.6; $p = 0.0067$) as the one between HV $\geq 70\%$ and malignancy (OR, 47.22; $p = 0.013$).

Strain Ratio	<1.5	≥1.5
Benign Lesions	15	0
Malignant Lesions	2	6

Table 1. Distribution of splenic lesions according to Strain ratio values and diagnosis

Hardness Value	<70%	≥70%
Benign Lesions	12	4
Malignant Lesions	0	8

Table 2. Distribution of splenic lesions according to Hardness values and diagnosis

Dog	Strain ratio	SD	Hardness Value	SD	Diagnosis
1	0,86	0,1	47,84	0,1	EE
2	1,07	0,11	32,72	8,99	EE
3	1,11	0,13	62,73	4,01	NI
4	1,45	0,07	69,65	0,65	NI
5	NC	NC	63	14,76	NI
6	0,95	0,04	32,47	1,82	NI
7	0,96	0,03	44	2	NI
8	0,87	0,03	19	4	NI
9	1,26	0,14	90,75	7,24	NI
10	0,93	0,1	37,55	12,54	NI
11	1,19	0,07	82,29	7,83	NI
12	1,3	0,15	83,76	9,16	NI
13	1,21	0,11	53,7	8,5	NI
14	1,11	0,11	69,87	16,14	NI
15	1,06	0,21	65,49	11,9	NI
16	1,26	0,08	98,44	1,29	NI
17	2,56	0,23	77,43	1,93	HSA
18	1,59	0,25	84,97	4,75	HSA
19	2,72	0,06	93,87	5	HSA
20	1,08	0,27	80,97	13,61	HSA
21	2,25	0,27	93,23	3,46	HSA
22	2	0,54	99,97	0,07	HSA
23	0,91	0,09	85,34	7,62	L
24	1,7	0,09	91,21	2,54	L

Table 3. Strain ratio and Hardness values of splenic lesions. SD: Standard deviation; EE: Extramedullary hematopoiesis; NI: Nodular Hyperplasia; HSA: Hemangiosarcoma; L: Lymphoma.

5.4 Discussion

The prevalence of benign versus malignant lesions in our sample (frequency respectively of 67% and 33%) is consistent with other studied about the same subject (Rossi, 2008; Hayes, 2012; Watson, 2011; Christensen, 2009; Ohlert, 2007; Cole, 2012). Nodular hyperplasia was the most represented lesion (13 of 24 lesions, 54%), while hemangiosarcoma was the most represented between malignant lesions (6 of 8, 75%). These results are also similar to those reported in other papers (Jun-Yong, 2012; Christenses, 2009; Watson, 2011). We observed that benign lesions tend to be as soft as the surrounding normal splenic parenchyma, while malignant lesions tend to be harder ($p < 0.05$) Figure 10.

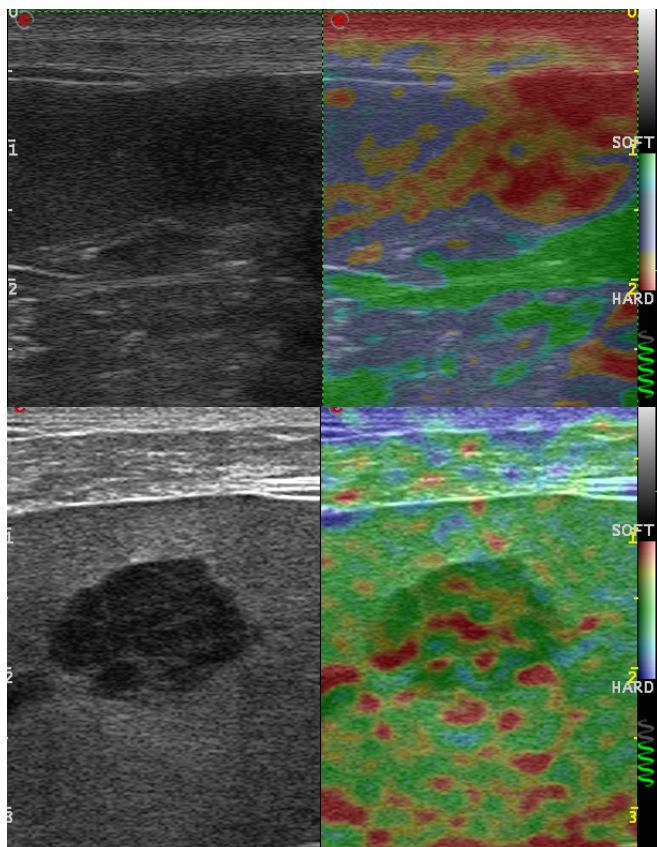


Figure 10: In the image above a malignant splenic lesion coded as harder than the normal surrounding splenic parenchyma; in the image below a benign splenic lesion coded as soft as the surrounding splenic parenchyma.

In our opinion the hardness of malignant lesions can be explained considering their high cells density, or in case of hemangiosarcoma their areas containing

fluids (incompressible for physics). All malignant lesions presented $HV \geq 70\%$ and 6 of 8 presented $SR \geq 1.5$. The 2 malignant lesions having $SR < 1.5$ were one lymphoma and one hemangiosarcoma and we can hypothesize that the necrotic and hemorrhagic areas in these tumors made the lesions softer and more deformable. All benign lesions presented a $SR < 1.5$ and 12 of 16 presented a $HV < 70\%$. The four of 16 benign lesions resulting harder than normal splenic parenchyma ($HV \geq 70\%$) were nodules of hyperplasia; these lesions may have many vessels containing, obviously, fluid that are incompressible and in our opinion made the lesion harder (Alder, 2013). Considering the HV our tests showed very high Se (100%) and a quite low Sp (75%); while considering SR a very high Sp (100%) and a quite low Se (75%). In our opinion these results can be due to the retrospective nature of our work that can contain some BIAS. However the value of $NLR < 0.1$ concerning HV hearten us and let us assert that this value can be useful in order to rule out the disease. Concerning the inter observer variability we obtained a $CV < 10\%$ (considering both value of SR and HV), that could be related to inherent variability of the technique as it requires repeated movements of compression and retraction of the probe as equal as possible between them. Concerning the intra-observer variability we obtained an overall very good agreement between operators considering both SR and HV. The low variability observed could depend on the different force applied by the two operators with the probe even considering that they tried to perform two compression of a few mm for each second. Considering OR we observed that a lesion presenting a $SR \geq 1.5$ or a $HV \geq 70\%$ has respectively almost 80 and 47 times more the possibility to be malignant than one with $SR < 1.5$ or $HV < 70\%$. There are some important limitation in this study. The work was retrospective and a small number of animals with a little lesions variation was considered. However this work represents an initial approach to the study of

splenic lesions in dogs using strain elastography. Further studies should also investigate the role of strain elastography in the monitoring of benign lesions that with time can turn into malignant and change their stiffness; or in the monitoring of those lesions that we cannot sample due to difficult situations. In conclusion real time elastography seems to be useful in differentiate malignant from benign splenic hypoechoic lesions less than 4 cm width. Lesions with $SR \geq 1.5$ have an high probability to be malignant while lesions with $HV < 70\%$ have a high probability to be benign. However the right way to reach a diagnosis cannot leave aside cytologic and/or histological evaluation.

CHAPTER 6

APPLICATION OF STRAIN ELASTOGRAPHY IN THE EVALUATION OF MAMMARY LESIONS IN DOGS

6. Application of Strain Elastography in the evaluation of mammary lesions in dogs

6.1 Introduction

The Shear Wave Elastography and the Strain Elastography are considered accurate methods in characterizing the nature of the woman's breast lesions (Barr, 2015).

In veterinary medicine there are a few reports describing the utility of the Shear wave Elastography in characterizing mammary lesions in dogs. These studies were briefly reported above in Chapter 4. To our knowledge there are no studies in veterinary medicine considering the role of Strain Elastography in characterizing canine mammary tumors. In women, breast lesions are classified according to: the Tsukuba Elasticity Score, the Elastogram-Bmode Ratio and the Lesion to fat ratio. Guidelines in human medicine recommend that the area of interest in SE images should include the subcutaneous tissue and the pectoral muscles. It should be as wide as possible; the ribs and lungs should not be included (Barr, 2015). According to Tsukuba (Tsukuba Elasticity Score) each lesion is scored, from 1 to 5, depending on the hardness displayed and the differences in size between the elastogram and B-mode:

- Score 1: elastic lesion
- Score 2: lesion with mixed pattern
- Score 3: hard lesion, smaller than the lesion in B-mode image
- Score 4: hard lesion of the same size of the B-mode image
- Score 5: hard lesion, bigger than the lesion in B-mode image

A biopsy is recommended for the lesions having score 4 or 5 (Itih, 2006); lesions scored 1-2-3 are classified as probably benign (Barr, 2015).

The Tsukuba score presented quite high values of sensitivity (86,5%), specificity (89,9%) and accuracy (88,3%) in differentiating breast masses in women (Itoh, 2006). The limits of this analytical method are the intra and inter-operator variability in assigning different scores (Barr, 2015). Other limitations affecting accuracy, may be related to the excessive size of some lesion and to their depth (Barr, 2015). Hall et al. (2003) found that the benign lesions on the elastogram appear smaller than the corresponding B-mode image (Elastogram/B-mode ratio), while the malignant ones appear larger. This is a feature seems to be typical of mammary tumors. On the basis of this study, the ratio between the diameter or the area of the lesion calculated on the elastogram and those calculated in B-mode has been proposed as a diagnostic criterion for differentiate breast cancer (Barr, 2010). Assuming ratios < 1 for benign lesions and ratios > 1 for malignant lesions a sensitivity of 100% and a specificity of 99% have been obtained. This ratio increases with the degree of malignancy (Barr, 2015). The Lesion to Fat ratio is a semiquantitative method that calculates the ratio between a region of interest included in the lesion and the subcutaneous adipose tissue. Malignant mammary lesions tend to have higher values than benign lesions (Zhou, 2014) presenting a sensitivity of 82,9% and a specificity of 75,6% . The aim of the study was to evaluate respectively whether the Strain Elastography is able to provide useful informations to differentiate the mammary tumors in bitches. According to our target, mammary lesions have been classified using the Tsukuba Elasticity Score and the elastogram/B-mode ratio. Finally the presence of invasiveness of the lesion was subjectively assessed considering the loss of delimitations on the elastogram. The results were then compared to the histological evaluation of each lesion.

6.2 Materials and Methods

Medical records belonging to dogs referred to our hospital, between January 2013 and December 2014, were evaluated in order to select all patients presented for ultrasound having one or more mammary tumors. All the ultrasonographic examinations were performed using an esaote MyLab 70 (Genova, Italy) equipped with a multifrequency linear transducer (7,5-13 MHz) in association with a Real-time Elastography module. Dogs were evaluated, after hair clipping and ultrasonographic gel applied, in right or left lateral recumbency in order to have the left or the right part of the abdomen upward (according to the localization of mammary lesions). Dogs underwent B-mode evaluation of the entire abdomen and elastosonographic evaluation of the mammary gland. Ultrasound examinations were performed by the same operator. Using the “dual screen mode” (for the simultaneous displaying of both the B-mode and elastosonographic images), a region of interest (ROI) has been selected, including the mammary lesion and the glandular parenchyma. The other anatomic structures such as ribs, the bladder or the great vessels were not included in the ROI. The elastogram was obtained applying a minimum vibration (Barr, 2015), with movements of retraction and compression carried out maintaining the ultrasonographic probe perpendicular to the skin surface. When the image was scanned correctly a green spiral appeared at the right bottom side of the screen. Images were acquired after at least 5 seconds lingering of the green spiral. In the elastogram hard areas (areas of low strain) were coded in blue, intermediate stiffness areas were coded in green and soft areas were coded in red (areas of high strain). Each mammary lesion was then classified according to the Tsukuba score, the presence /absence of infiltration on the elastogram and to the elastogram/B-mode ratio.

The Tsukuba score was interpreted as follows:

- Score 1: lesion presenting > 50% of area coded as soft with rare hard foci
- Score 2: lesion presenting > 50% of area coded as soft with some hard focal areas
- Score 3: lesion presenting > 50% of area coded as hard located at the core of the nodule without reaching the lesions limits
- Score 4: lesion presenting > 50% of area coded as hard with some hard areas reaching the lesions limits
- Score 5: lesion presenting > 50% of area coded as hard reaching the lesions limits

The lack of demarcation between the lesions margins and the surrounding soft tissue was considered as elastosonographic infiltration. Where the lesions limits were not defined, the neoplasm appeared in continuity with the surrounding soft tissue. The difference in size between the lesion scanned in B-mode and at the elastogram (elastogram/B-mode ratio) was evaluated subjectively, visually comparing the lesions amplitude in the two different images. The tumors were classified into two groups: lesions that appear larger (or of equal size) at the elastogram than on the B-mode and lesions that appear smaller. Each mammary lesion underwent to histological examination (after mastectomy) or cytological examination (fine needle aspiration).

The Pearson's chi-square test was used to assess the presence of a statistically significant difference between the benign or malignant tumors according to the Tsukuba score results. The Fisher's exact test was used to assess the presence of statistically significant difference between the benign or malignant tumors according to the elastogram/B-mode ratio. Values of $p \leq 0,05$ were considered significant. The K of Cohen was used to verify the agreement between the elastosonographic assessment of infiltration and the

histological confirmation of tumors invasion. K values were considered as follows:

- $k=0$: no agreement
- $k=0-0,4$: poor agreement
- $k=0,4-0,6$: medium agreement
- $k=0,6-0,8$: good agreement
- $k=0,8-1$: perfect agreement

6.3 Results

Our population included 21 dogs (20 bitches presenting a single mammary lesion and 1 presenting five nodules.): 1 Pinscher, 1 Maremma Shepherd, 3 German Shepherds, 2 Dachshund, 2 Jack Russell terrier, 2 English Cocker Spaniel, 1 Shar-Pei, 1 Shetland Sheepdog, 1 Bergamasco, 1 Italian Bracco, 1 Yorkshire terrier, 1 Rottweiler, 4 mongrel. Twenty-five lesions were analyzed. The age of bitches at the time of the study ranged from 5 to 14 years, with an average value of 9.76 years. Only 4 of 21 bitches were neutered. There were no bitch in lactation. Lesions size ranged from 2 mm to 8 cm. The elastosonographic examination was feasible in all cases. Twenty-four lesions underwent histological examination, on 1 lesion underwent cytology. Eight lesions resulted benign while 15 malignant. A lesion was classified as intra-ductal papilloma with initial carcinomatous evolution and was thus classified as a malignant lesion. The only lesion evaluated by cytology presented epithelial cells showing moderate signs of malignancy and it was thus considered as malignant. Table 4 shows the localization and the final diagnosis of the 25 lesions. No lesion appeared to be softer than the surrounding soft tissues. Table 5 shows the number of lesions classified according to the Tsukuba score. The Pearson's chi-square test did not

reported significant differences between groups (chi-square= 5,09; degrees of freedom= 4, p=0,278). Considering the assessment of the elastosonographic infiltration it was not possible to classify 3 lesions (2 lesions because of the poor quality of images and 1 because of the cytological origin of the diagnosis). Twelve lesions out of 22 presented infiltrated margins at the elastogram while 10 did not. Table 6 shows the result of the infiltration assessment in correlation to the histological examination. The K of Cohen presented a value of 0,384 corresponding to a poor agreement. The results obtained are reported: 15 agreement (68,18% of the total observations); 10 agreement expected by chance (48,35% of the total observations); K sensibility 0,174; confidence interval 95% from 0,044 to 0,724. The assessment of the elastogram/B-mode ratio was not possible.

DOG	AGE	SEX	MAMMARY GLAND AFFECTED	DIAGNOSIS
1	8 yo	F	III	adenocarcinoma
2	10 yo	F	IV	papilloma with carcinomatous evolution
3	10 yo	F	IV	adenocarcinoma
4	10 yo	F	IV	adenocarcinoma
5	10 yo	NF	III	lobular hyperplasia
6	11 yo	NF	II	adenoma
7	11 yo	F	II	adenocarcinoma
8	5 yo	F	V	adenocarcinoma
9	14 yo	F	V (left)	adenocarcinoma
			V (right)	ductal ectasia
			IV	adenocarcinoma
			III	adenocarcinoma
			II	normal gland
10	7 yo	F	IV	myoepithelioma
11	9 yo	F	III	adenocarcinoma
12	11 yo	NF	II	carcinoma
13	6 yo	F	III	adenocarcinoma
14	11 yo	F	IV	adenocarcinoma
15	8 yo	F	IV	condroma
16	13 yo	F	between IV and V	adenocarcinoma
17	9 yo	F	V	adenocarcinoma
18	9 yo	F	IV	mixed benign tumor
19	9 yo	F	iii	adenoma
20	14 yo	F	V	adenocarcinoma
21	10 yo	NF	i	carcinoma

Table 4. Distribution of mammary lesions according to sex and age. yo: years old; F: female; NF: neutered female.

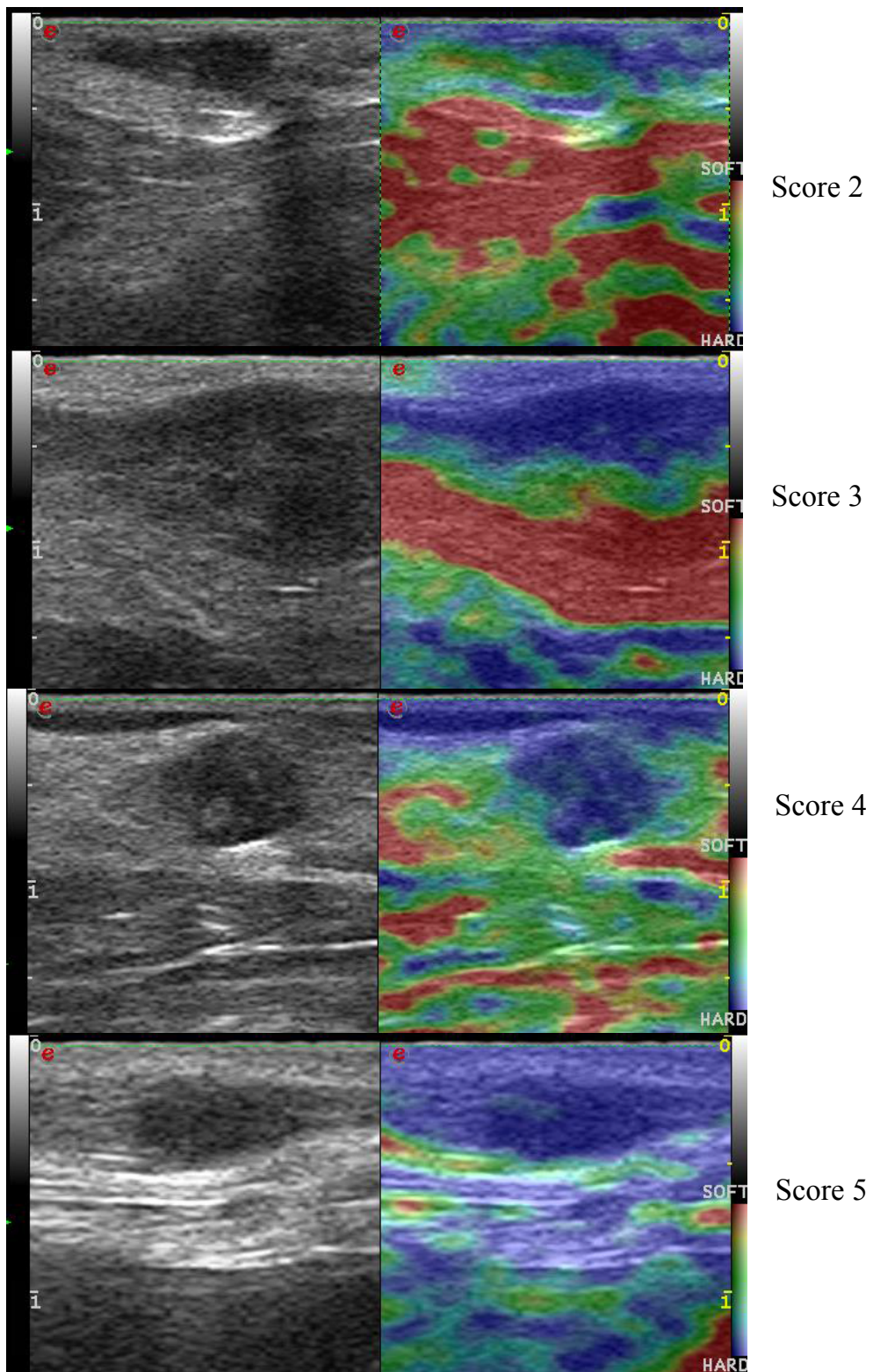


Figure 11. Examples of lesion classified in the different Tsukuba scores (from 2 to 5). From the top to the bottom: Ductal Ectasia - Adenoma - Adenocarcinoma - Adenocarcinoma

LESION	SCORE 1	SCORE 2	SCORE 3	SCORE 4	SCORE 5	TOTAL
BENIGN	0	2	2	2	2	8
MALIGNANT	0	2	1	9	5	17
TOTAL	0	4	3	11	7	25

Table 5. Number of mammary lesions according to Tsukuba score

LESIONS MARGINS	INFILTRATION HISTOLOGICALLY CONFIRMED	INFILTRATION HISTOLOGICALLY NOT CONFIRMED	TOTAL
INFILTRATED ON ELASTOGRAM	6	6	12
NOT INFILTRATED ON ELASTOGRAM	1	9	10
TOTAL	7	15	22

Table 6. Number of mammary lesions according to the elastosonographic and histological infiltration assessment.

6.4 Discussion

The bitches considered in our study presented a medium age value of 9,76 years close to that reported in literature of 10-11 years (Lana, 2007). Lana (2007), reported that the caudal mammary glands (IV and V), appear to be the most affected by mammary tumors; in agreement with this finding in our study 14 lesions were located at the IV and V mammary glands. We reported a low rate of malignant lesions (32%) compared to literature (Queiroga, 2002). The Strain Elastography was easily applied to every lesion. However the Tsukuba score did not appear to be a reliable interpretation technique in differentiating mammary neoplasia. Our results are in conflict with those reported in human literature concerning the application of this scoring system in the analysis of breast cancer (Itoh, 2006), having in women a sensitivity

and specificity of 86.5% and 89.9%. Analyzing the scores attributed to benign neoplasms in our study, we can see that these tumors are equally classified in scores ranging from 2 to 5: 2 lesions were classified with scores 2, 2 with score 3, 2 with score 4, 2 with score 5. Malignancies had heterogeneous distribution: 2 have been cataloged with score 2, 1 with score 3, 9 with score 4, 5 with score 5. No lesion was cataloged with score 1. We can explain our results basing on some considerations reported below.

Qualitative variability of the parenchyma surrounding the lesion

Strain elastography provides qualitative and relative results: the elasticity described in the elastogram is not calculated basing on the absolute stiffness of the tissue but on its deformation in relation to the surrounding tissue. For this reason it is of fundamental importance that the surrounding parenchyma present mechanical characteristics as much constant as possible. Both the human breast tissue that the canine mammary tissue can vary. The mammary parenchyma in dogs, however, is the most variable. As women breast it can be subjected to changes according to age, hormonal status or functional phase (lactation). Similar to the human species there are some inter-individual differences determined by breed differences. Ovariectomy and ovariectomy are influencing conditions. Bitches, instead of women, often underwent spaying surgery; gonadectomy modify the hormonal status of the subject changing the morphological characteristics of the mammary gland. This change can be consistent with the age of subject at the time of surgery. We can list also some inter-individual differences that are present in dogs. Bitches present five pair of mammary glands, distributed on ventral parte of the abdominal surface (2 or 3 thoracic glands and 2-3 inguinal glands). This difference imply some anatomical and structural differences. In the inguinal region, usually we can find more subcutaneous fat tissue than in the thoracic

or axillary region. This tissue is included in the glandular structure, and having different mechanical characteristics can modify the compressibility of the mammary gland (in which the lesion is located). Usually the two/three pairs of cranial mammary glands are vascularized by the thoracic lateral artery, the cranial epigastric superficial artery and branches of the intercostal arteries. The two/three pairs of caudal mammary glands are vascularized by the caudal superficial epigastric artery and the branches of the caudal abdominal, deep circumflex and iliac arteries. The venous path follows the arterial one. The axillary lymph nodes drain the I and II thoracic glands while the superficial inguinal lymph nodes the IV and V; the third breast can be drained by one or the other. Fluids are physically incompressible and at the elastosonographic examination they can affect compressibility of tissue. Thus the different vascular path of the thoracic and inguinal mammary gland can imply some difference in compressibility. It can be difficult to assess the elasticity of a soft lesion surrounded by a hard parenchyma, since the peripheral parenchyma acts as a hard shell that prevents the generation of strain within the lesion itself (eggshell effect). This situation might be found during mastitis or hyperplastic processes changing the mechanical characteristics of the mammary tissue.

Localization of tumors in dogs

In addition to the greater qualitative variability, the mammary glands of bitches, were different from those of women, even on a quantitative level. The human mammary tumors are generally entirely included in the parenchyma. The lesions object of our study are often superficial, sometimes in continuity with the skin and not totally surrounded by breast tissue. The reason for this difference may be due to the lower quantity of mammary tissue which is generally present in bitches, especially if these are not lactating. The limited

glandular parenchyma, which does not extend in depth and does not constitute a layer of substantial thickness, would result in a superficial location of neoplasms. The superficiality of the tumors was considered a factor negatively influencing the accuracy of the application of Strain elastography also in human medicine (Barr, 2015). In addition some lesions in our sample were in contact or close to the skin and represented in our opinion a source of inaccuracy. The skin generally appears as a hard structure thus: if a hard lesion is immersed in the glandular healthy tissue it will be easily definable, if instead it is in contact with a tissue of comparable hardness, its margins will not be distinguishable. The complex skin-lesion may have been regarded as a single lesion, with an high score according Tsukuba (Figure 12).

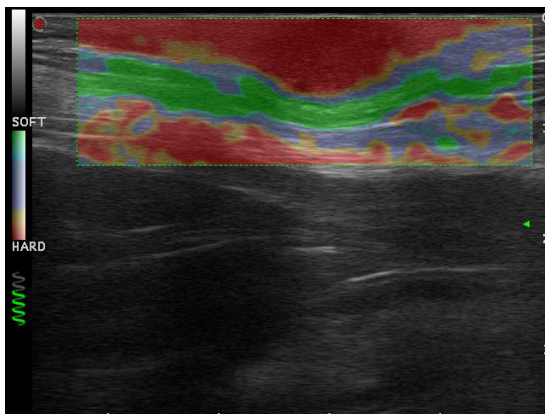


Figure 12. Examples of a complex skin-lesion (Adenocarcinoma). Lesions limits are not distinguishable.

Two-dimensional analysis of a three-dimensional structure

With the elastosonographic analysis we can obtain two-dimensional scanning of three-dimensional structures. It is possible that the tumors in our study were examined by analyzing scanning planes that did not provided portions of tissue sufficiently representative. For example a malignant lesions could have been scanned at its necrotic portion appearing soft or a benign lesion could have been scanned at its fibrosclerosis areas appearing hard. We can also consider that some mammary lesions in dogs can evolve from benign to

malignant. The scanned portion of these tumors may be responsible of the elastosonographic result; showing or not the real evolutionary trend (Figure 13).

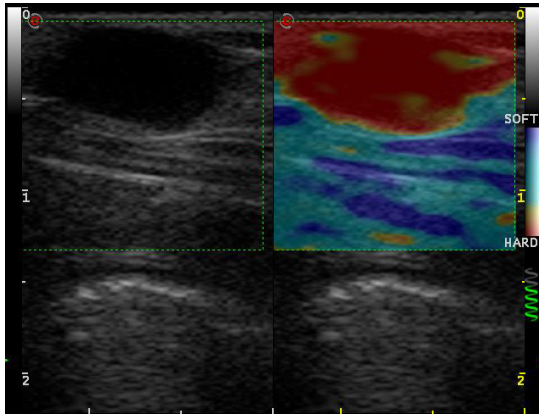


Figure 13. Intraductal papilloma with initial carcinomatous evolution classified in score 5.

Mechanical characteristics of the lesion

It may be possible that there were errors in the classification of lesions due to their mechanical characteristics. Malignant lesions may be classified as soft if within them there were extensive areas of necrosis (compressible areas). Both cases of malignant lesions in pur sample classified with score 2 were tubular complexes adenocarcinomas with necrotic centers (Figure 14).

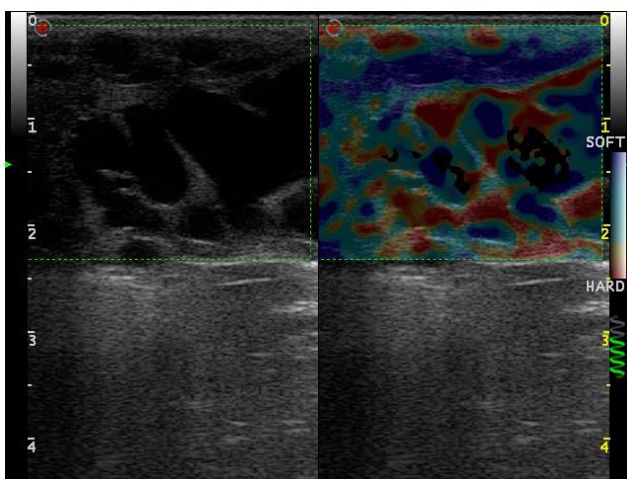


Figure 14. Tubular complex adenocarcinoma with necrotic centers classified in score 2.

As reported by Glinska-Suchocka et al. (2013), if we analyze a benign mixed tumor in which cartilaginous or bone tissue are present, the hardness of the lesion may be high and this could lead to misinterpretation. Similarly it could happen if an extended process of desmoplasia is present in a benign tumor (Glinska-Suchocka, 2013). In our study a tubular simple adenoma characterized by intense desmoplasia and classified with score 4 (Figure 15).

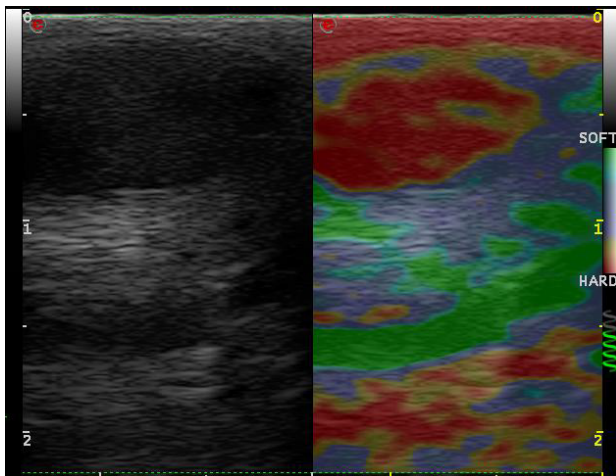


Figure 15. Tubular simple adenoma with desmoplasia classified in score 4.

The ultrasound device used in this study (Esaote MyLab 70), does not display the cystic structures with artifacts (BGR or Bull's Eye Artifact). It can therefore be assumed that benign lesions containing cysts could be evaluated as hard, considering the incompressibility of fluids. A cystic tubular adenoma circumscribed by thick capsule in this study has been classified with score 4 (Figure 16).

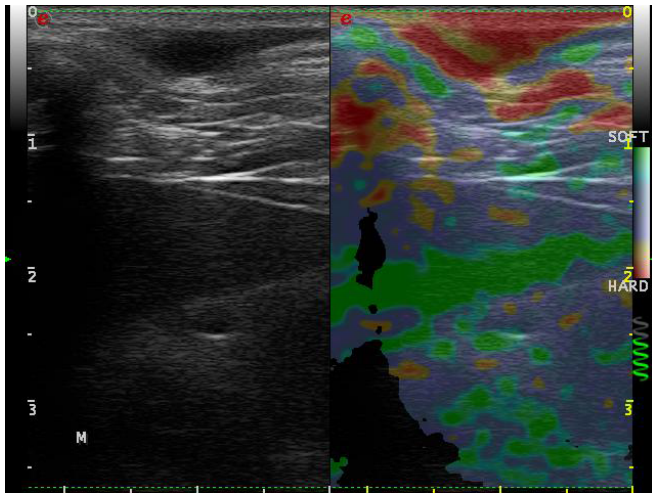


Figure 16. Cystic tubular adenoma circumscribed by thick capsule in this study has been classified with score 4

The presence-absence of elastosonographic infiltration not emphasized statistically significant differences between lesions whose margins appeared histologically infiltrating or not infiltrating. We found 6 false positive and one false negative. The qualitative variability of the parenchyma surrounding the lesion may have led to cases of false positivity. Even in this type of analysis, in fact, peripheral areas that appear elastosonographically hard and in continuity with the lesion, may have been interpreted as areas of infiltration. Similarly, the location of tumors in dogs, usually located, as mentioned before, in a superficial position, may have led to false positives. This could be explained considering that the hardness continuity between the lesion and the skin was wrongly interpreted as infiltration. Considering again that we carried out a two-dimensional analysis of a three-dimensional structure, it can be possible that we scanned portions of the neoplasms in which the infiltration is not present (leading to false negative). In other cases it is possible that a limited infiltration area, viewable only microscopically, cannot produce a change of the mechanical characteristics of the tissue and so cannot be elastosonographically detected. The classification of the mammary lesions based on the difference in size between the lesion at the elastogram and at the B-mode was not executable. This inapplicability can be explained considering

the polymorphism of mammary tumors in our study. The woman's mammary tumors described in literature generally appear round regular shaped at the elastogram; their margins and then their size are well evaluated. The lesions in our study had often irregular margins, sometimes not well defined; their form was variable and sometimes not outlineable. These features made not possible to evaluate the size of the lesions at the elastogram. In addition to a hypothetical higher polymorphism of mammary cancer in dogs, we assume that the qualitative variability of the parenchyma surrounding the lesion and the particular location of the tumors themselves, already mentioned, they could have contributed to the non-definable margins. In the present study a palpable lesion was not viewable in the B-mode analysis, but it was localized using the elastosonographic examination. The lesion appeared particularly extensive in the B-mode image instead, at the elastogram in the context of this structure there was a well-defined lesion of the same size of the palpated area (Figure 17). This lesion was a simple tubular adenocarcinoma.

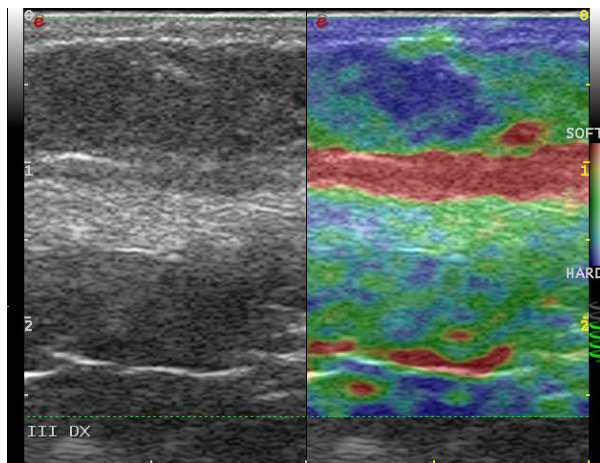


Figure 17. A palpable lesion not distinguishable at the B-mode examination but clearly viewable at the elastogram. Simple tubular carcinoma classified in score 4.

It would be interesting for future studies to evaluate the usefulness of Strain Elastography to detect very small lesions, non-palpable, as well as non-displayable to the B-mode. This study appears to be in disagreement with the reports of Glinska-Suchocka et al. (2013) and Feliciano et al. (2014). These

works described the useful application of Shear wave elastography and ARFI elastography in the study of mammary neoplasms in bitches. Both the authors reported statistically significant differences between the elastographic pattern of benign and malignant lesions. However it should be stressed that the techniques used in the two studies (based on shear waves; purely technical and quantitative) are different from that applied in our work. Their results are not affected by the variability of the tissue surrounding the lesion that instead affects Strain elastography. A starting point for future strain elastography studies, in order to avoid this variability, should be the selection of dogs of similar age, of the same size, of the same estrous phase and having tumors of the same mammary gland. This new study should be prospective, based on elastosonographic examination of lesions including several scanning plans. Our study analyzed a relatively small number of cases; it should be useful to comprise much more cases presenting also the same number of benign and malignant lesions. Following studies could then be set in consideration of the possible mistakes made in this study. However, evaluating a study it would also be appropriate to consider the possible clinical significance. A report that present no significant results may have more importance than one whose data are statistically significant. Roush (2015) points out that often a study is evaluated paying much attention to his "statistical power", ignoring if statistical significance can lead to clinical significance. Greatly expanding the number of cases studied, it will always be possible to find small differences resulting in statistically significant results. Even Houle (2008) highlighted the inutility of many studies showing statistically significant results but an absolute clinical irrelevance. Finally the Strain Elastography was as an applicable technique in evaluating mammary neoplasms in our sample, demonstrating their elastographic patterns; but it was clinically not useful in differentiating benign from malignant lesions.

CHAPTER 7

APPLICATION OF STRAIN ELASTOGRAPHY IN THE EVALUATION OF SUPERFICIAL LESIONS IN DOGS: COMPARING TWO SCORE SYSTEMS

7. Application of Strain Elastography in the evaluation of superficial lesions in dogs: comparing two score systems

7.1 Introduction

In veterinary medicine the ultrasonographic examination of the skin and subcutaneous soft tissue is performed for the evaluation of superficial nodules/masses and swellings. High frequency linear transducers (at least 10-15 MHz) are used to study the superficial layers of the body and to distinguish the lesions may be present in them. The normal appearance of the superficial soft tissue depend on: the localization, the state of hydration/nutrition and body condition score of the animal. Usually, the ultrasound examination allows the identification of the epidermis, dermis, subcutaneous tissue, musculoskeletal system and abdominal or thoracic wall/ribs (depending on body region). Ultrasound can be useful in the identification of a cutaneous/subcutaneous nodule and in the estimation of its dimensions, shape and limits. Doppler evaluation can be used to certify the vascularization and distribution of blood vessels in a lesion. However the sonographic appearance of a superficial nodule can often be non-specific and a cytologic or histologic evaluation in needed.

Cytological examination is generally the first choice because it is less expensive than histology, rapid in execution, not invasive and more rapid in reading and reporting, it does not require patients sedation and allows an accurate diagnosis (Cohen, 2003). The cytological evaluation presents anyway some limits: it may be inconclusive because of the poor quality of or the low cellularity of the sample due to incorrect manuality or due to the biological characteristics of the tissue sampled (Simenov, 2012). In veterinary medicine a few studies prove the accuracy of cytological diagnosis of

superficial lesions resulting in a sensitivity and a specificity of 89-90% and 100-97% respectively (Chalita, 2001; Radostin, 2012). The correlation between cytological and histological diagnosis of superficial lesions has proven to be very high (88-90%). (Ghisleni, 2006; Simenov 2012).

The use of Strain elastography in the evaluation of superficial lesions in dogs has not been reported yet. The aim of this research was to evaluate:

- the application of strain elastography in the evaluation of superficial lesions in dogs;
- the role of strain elastography in differentiate malignant from benign lesions basing of a score system obtained after objective measurements calculated by an integrated software;
- the agreement between the subjective visual evaluations of three operators (expressed in score system) and the objective score calculated for each lesions by an integrated software;
- the agreement between the score systems obtained by each operator for the same lesions.

7.2 Materials and methods

Sixty nodular skin lesions from 36 canine patients were evaluated in this retrospective study, conducted from May 2013 to February 2015 . Only nodules with a final diagnosis, obtained by cytology and/or histology were considered. Mammary lesions or nodules located in the mammary region were not considered. All the ultrasonographic examinations were performed using an esaote MyLab 70 (Genova, Italy) equipped with a multifrequency linear transducer (7,5-13 MHz) in association with a Real-time Elastography module. Dogs were evaluated, after hair clipping and ultrasonographic gel applied, in right or left lateral recumbency in order to have the left or the right part of the abdomen upward (according to the localization of the superficial

lesion). Ultrasound examinations were performed by three operators in sequence. Using the “dual screen mode” (for the simultaneous displaying of both the B-mode and elastosonographic images), a region of interest (ROI) has been selected, including the superficial lesion and an area of normal parenchyma. The other anatomic structures such as ribs, the bladder or the great vessels were not included in the ROI. The elastogram was obtained applying a minimum vibration (Barr, 2015), with movements of retraction and compression carried out maintaining the ultrasonographic probe perpendicular to the skin surface. When the image was scanned correctly a green spiral appeared at the right bottom side of the screen. Images were acquired after at least 5 seconds lingering of the green spiral. Five images were obtained for each lesion. In the elastogram hard areas (areas of low strain) were coded in blue, intermediate stiffness areas were coded in green and soft areas were coded in red (areas of high strain). Superficial lesions were sampled right after the elastosonographic exam (cytology or histology). In order to prove the accuracy of the score system, an operator measured the real hardness value of each lesion using a measurements software provided by the manufacturer and integrated in device MyLab 70. The software measured the percentage of hard area included in the lesion and color classified as heavy-blue areas (Figure 18).

These objective measurements were turned into 2 score systems:

SCORE 1

- Grade 1: lesion presenting > 80% of area coded as soft
- Grade 2: lesion presenting > 50% but < 80% of area coded as soft
- Grade 3: lesion presenting > 50% but < 80% of area coded as hard
- Grade 4: lesion presenting > 80% of area coded as hard

SCORE 2

- Grade 1: lesion presenting < 10% of area coded as hard
- Grade 2: lesion presenting > 10% but < 40% of area coded as hard
- Grade 3: lesion presenting > 40% but < 60% of area coded as hard
- Grade 4: lesion presenting > 60% bot < 90% of area coded as hard
- Grade 5: lesion presenting > 90% of area coded as hard

Each lesion has been classified, subjectively by each one of the three operators, according to two different score systems. Any operator was aware of the patients signalment, real hardness value of the lesion in exam and its final diagnosis.

The K of Cohen was used to verify the agreement between the elastosonographic assessment of the three operators. K values were considered as follows:

- k=0: no agreement
- k=0-0,4: poor agreement
- k=0,4-0,6: medium agreement
- k=0,6-0,8: good agreement
- k=0,8-1: perfect agreement

The Student t-test was used to assess whether there was a statistically significant difference between benign/malignant considering the hardness value calculated using the software. The Pearson chi-square test was used to assess the existence of statistically significant differences between benign and malignant lesions considering the two score proposed above. Values of $p < 0,05$ were considered significant.

7.3 Results

The mean age of dogs in the present study was 8 years old (from 3 to 13 years old); 18 dogs were male and 18 females. Canine breeds included were: American Staffordshire Terrier, Beagle, English Setter, Jack Russel Terrier, French Bulldog, Golden Retriever Labrador Retriever, Mongrel, Pug, Sharpei, Shetland Sheepdog, Shih-tzu, Yorkshire Terrier. The diagnosis and method of assessment of each lesion is reported in Table 7. Thirty seven of 60 lesions (62%) were malignant while 23 of 60 were benign (38%). The hardness value obtained by the software measurements for each lesion is reported in Table 8 together with the correspondent Grade according to the Score system 1 and 2.

CASE	EXAM	DIAGNOSIS
1	HISTOLOGY	SARCOMA
2	HISTOLOGY	SARCOMA
3	CITOLOGY	PANNICOLOTIS
4	CITOLOGY	MAST CELL TUMOR
5	CITOLOGY	LYPOMA
6	CITOLOGY	MAST CELL TUMOR
7	HISTOLOGY	MAST CELL TUMOR
8	CITOLOGY	PANNICOLITIS
9	HISTOLOGY	MAST CELL TUMOR
10	HISTOLOGY	MAST CELL TUMOR
11	CITOLOGY	HUMBILICAL HERNYA
12	CITOLOGY	BENIGN FOLLICULAR NEOFORMATION
13	CITOLOGY	BENIGN FOLLICULAR NEOFORMATION
14	HISTOLOGY	MAST CELL TUMOR
15	HISTOLOGY	MAST CELL TUMOR
16	HISTOLOGY	MAST CELL TUMOR
17	HISTOLOGY	SEBACEOUS CYST
18	CITOLOGY	MAST CELL TUMOR
19	CITOLOGY	MAST CELL TUMOR
20	CITOLOGY	MAST CELL TUMOR
21	CITOLOGY	MAST CELL TUMOR
22	CITOLOGY	MAST CELL TUMOR
23	HISTOLOGY	MAST CELL TUMOR
24	HISTOLOGY	LYPOMA
25	HISTOLOGY	LYPOMA
26	HISTOLOGY	PHLOGOSIS
27	HISTOLOGY	TRANSMISSIBLE VENEREAL TUMOR
28	CITOLOGY	LYPOMA

CASE	EXAM	DIAGNOSIS
29	CITOLOGY	LIPOMA
30	HISTOLOGY	LIPOMA
31	CITOLOGY	SARCOMA
32	CITOLOGY	LIPOMA
33	CITOLOGY	MAST CELL TUMOR
34	CITOLOGY	LIPOMA
35	CITOLOGY	LYMPHOMA
36	CITOLOGY	LYMPHOMA
37	CITOLOGY	BENIGN FOLLICULAR NEOFORMATION
38	HISTOLOGY	MAST CELL TUMOR
39	HISTOLOGY	MAST CELL TUMOR
40	HISTOLOGY	MAST CELL TUMOR
41	CITOLOGY	MAST CELL TUMOR
42	CITOLOGY	MAST CELL TUMOR
43	CITOLOGY	MAST CELL TUMOR
44	CITOLOGY	MAST CELL TUMOR
45	CITOLOGY	KERATIN CYST
46	CITOLOGY	LYMPHOMA
47	CITOLOGY	MAST CELL TUMOR
48	CITOLOGY	MAST CELL TUMOR
49	CITOLOGY	MAST CELL TUMOR
50	CITOLOGY	MAST CELL TUMOR
51	CITOLOGY	MAST CELL TUMOR
52	HISTOLOGY	MAST CELL TUMOR
53	HISTOLOGY	MAST CELL TUMOR
54	HISTOLOGY	MAST CELL TUMOR
55	CITOLOGY	LIPOMA
56	CITOLOGY	LIPOMA

CASE	EXAM	DIAGNOSIS
57	CITOLOGY	LIPOMA
58	CITOLOGY	PHLOGOSIS
59	HISTOLOGY	PHLOGOSIS
60	HISTOLOGY	PHLOGOSIS

Table 7. Classification and diagnosis of each lesion.

CASE	H.VALUE	SCORE 1	SCORE 2	CASE	H.VALUE	SCORE 1	SCORE 2
1	83,96	4	4	31	38,37	2	2
2	97,32	4	5	32	26,93	2	2
3	20,47	2	2	33	39,55	2	2
4	44,26	2	3	34	18,28	1	2
5	60,67	3	4	35	91,8	4	5
6	48,24	2	3	36	80,36	4	4
7	11,15	1	2	37	38,22	2	2
8	21,91	2	2	38	81,68	4	4
9	63,76	3	4	39	81,83	4	4
10	92,06	4	5	40	98,25	4	5
11	22,87	2	2	41	99,55	4	5
12	33	2	2	42	100	4	5
13	23,79	2	2	43	55,73	3	3
14	87,82	4	4	44	75,08	3	4
15	91,52	4	5	45	69,05	3	4
16	97,67	4	5	46	26,42	2	2
17	68,54	3	4	47	30,63	2	2
18	78,42	3	4	48	57,04	3	3
19	94,42	4	5	49	54,78	3	3
20	88,23	4	4	50	65,5	3	4
21	59,33	3	3	51	74,51	3	4
22	71,6	3	4	52	64,99	3	4
23	100	4	5	53	55,16	3	3
24	28,9	2	2	54	15,3	1	2
25	9,15	1	1	55	38,9	2	2
26	99,6	4	5	56	16,49	1	2
27	73,97	3	4	57	10,94	1	2
28	19	1	2	58	13,18	1	2

CASE	H.VALUE	SCORE 1	SCORE 2	CASE	H.VALUE	SCORE 1	SCORE 2
29	32,33	2	2	59	65,13	3	4
30	37,31	2	2	60	70,79	3	4

Table 8. Hardness value of each lesions and its corresponding Grade according to Score system 1 and 2.

CASE	OP. 1	OP. 2	OP. 3	CASE	OP. 1	OP. 2	OP. 3
1	4	4	4	31	2	2	2
2	4	4	4	32	1	1	2
3	1	1	1	33	2	2	2
4	2	2	2	34	1	1	1
5	1	1	2	35	4	4	4
6	3	3	2	36	4	4	3
7	1	1	1	37	2	2	2
8	1	1	1	38	4	4	4
9	4	3	4	39	4	4	4
10	4	4	4	40	4	4	3
11	1	1	1	41	4	4	4
12	2	2	2	42	4	4	4
13	2	2	2	43	2	3	3
14	4	4	4	44	4	4	3
15	4	4	4	45	3	3	3
16	4	4	4	46	1	1	1
17	3	3	3	47	1	1	1
18	4	4	4	48	2	2	2
19	4	4	4	49	3	3	3
20	4	4	4	50	3	2	3
21	4	4	3	51	4	3	4
22	4	4	3	52	4	4	4
23	4	4	4	53	3	2	3
24	2	1	2	54	1	1	2
25	1	1	2	55	2	2	2
26	4	4	4	56	1	1	1
27	3	4	4	57	1	1	1
28	1	1	1	58	1	1	1

CASE	OP. 1	OP. 2	OP. 3	CASE	OP. 1	OP. 2	OP. 3
29	2	2	2	59	3	4	3
30	1	1	1	60	3	4	3

Table 9. Classification of each lesions according to each single operators point of view for Score 1.

The classification of each lesions according to each single operators point of view are recorded in Table 9 for Score 1 and Table 10 for Score 2.

CASE	OP. 1	OP. 2	OP. 3	CASE	OP. 1	OP. 2	OP. 3
1	5	5	4	31	2	2	2
2	5	5	5	32	2	2	1
3	1	2	1	33	2	2	2
4	2	3	2	34	1	1	1
5	2	2	2	35	4	5	5
6	3	3	3	36	4	4	4
7	1	1	1	37	2	2	2
8	1	2	1	38	4	5	5
9	5	4	4	39	5	5	5
10	5	5	5	40	5	5	5
11	1	2	1	41	5	5	5
12	2	2	2	42	5	5	5
13	2	2	3	43	3	3	3
14	5	5	5	44	4	4	3
15	5	5	5	45	4	4	4
16	5	5	5	46	2	2	1
17	3	4	4	47	2	2	1
18	4	4	4	48	2	2	2
19	5	5	5	49	4	4	3
20	5	5	5	50	4	3	3
21	4	4	3	51	5	4	4
22	5	5	4	52	5	4	4
23	5	5	5	53	3	3	3
24	2	2	1	54	2	2	1
25	2	2	1	55	2	2	2
26	5	5	5	56	1	1	1
27	4	4	4	57	2	2	1
28	1	2	1	58	1	1	1

CASE	OP. 1	OP. 2	OP. 3	CASE	OP. 1	OP. 2	OP. 3
29	2	2	2	59	4	4	4
30	2	2	1	60	3	4	4

Table 10. Classification of each lesions according to each single operators point of view for Score 2. OP: Operator

The distribution of lesions according to score and malignancies are reported in Table 11 for score 1 and Table 12 for score 2.

SCORE	MALIGNANT	BENIGN	TOTAL
1			
Grade 1	2 (25%) 2 Mast cell tumor	6 (75%) 5 Lipoma 1 Phlogosis	8
Grade 2	6 (35%) 4 Mast cell tumor 1 Lymphoma 1 Sarcoma	11 (65%) 5 Lipoma 3 Benign Follicular Neoformation 2 Panniculitis 1 Umbilical Hernia	17
Grade 3	13 (72%) 12 Mast cell tumor 1 Transmissible Venereal Tumor	5 (28%) 2 Phlogosis 1 Lipoma 1 Keratin Cyst 1 Sebaceous Cyst	18
Grade 4	16 (94%) 12 Mast cell tumor 2 Lymphoma 2 Sarcoma	1 (6%) 1 Phlogosis	17
TOTAL	37	23	60

Table 11. Distribution of lesions in Score 1. The percentage of benign and malignant lesions are reported according to diagnosis.

SCORE	MALIGNANT	BENIGN	TOTAL
2			
Grade 1	0	1 (100%) 1 Lipoma	1
Grade 2	6 (27%) 4 Mast cell tumor 1 Lymphoma 1 Sarcoma	16 (73%) 9 Lipoma 3 Benign Follicular Neoformation 2 Panniculitis 1 Phlogosis 1 Umbilical Hernia	22
Grade 3	7 (100%) 7 Mast cell tumor	0	7
Grade 4	14 (74%) 11 Mast cell tumor 1 Lymphoma 1 Sarcoma 1 Transmissible Venereal Tumor	5 (26%) 2 Phlogosis 1 Lipoma 1 Keratin Cyst 1 Sebaceous Cyst	19
Grade 5	10 (91%) 8 Mast cell tumor 1 Lymphoma 1 Sarcoma	1 (9%) 1 Phlogosis	11
TOTAL	37	23	60

Table 12. Distribution of lesions in Score 2. The percentage of benign and malignant lesions are reported according to diagnosis.

The results of the agreements degree between the operators measurements concerning each score are reported in the tables below.

The K values in tables 13, 14 and 15 refer to Score 1; the K values in tables 16,17 and 18 refer to Score 2.

	Operator 2					
Operator 1		Grade 1	Grade 2	Grade 3	Grade 4	TOTAL
	Grade 1	16	0	0	0	16
	Grade 2	1	8	1	0	10
	Grade 3	0	2	5	3	10
	Grade 4	0	0	2	22	24
	TOTAL	17	10	8	25	60

Table 13. Agreement between Operator 1 and Operator 2 concerning Score 1.

K=0,788 good agreement

Standard error for K=0,064

Weighted K=0,891 very good agreement

	Operator 1					
Operator 3		Grade 1	Grade 2	Grade 3	Grade 4	TOTAL
	Grade 1	12	0	0	0	12
	Grade 2	4	10	1	0	15
	Grade 3	0	1	7	5	13
	Grade 4	0	0	1	19	20
	TOTAL	16	11	9	24	60

Table 14. Agreement between Operator 3 and Operator 1 concerning Score 1.

K=0,728 good agreement

Standard error for K=0,069

Weighted K=0,849 very good agreement

	Operator 2					
Operator 3		Grade 1	Grade 2	Grade 3	Grade 4	TOTAL
	Grade 1	12	0	0	0	12
	Grade 2	5	9	1	0	15
	Grade 3	0	2	4	7	13
	Grade 4	0	0	4	16	20
	TOTAL	17	11	9	23	60

Table 15. Agreement between Operator 3 and Operator 2 concerning Score 1.

K=0,570 moderate agreement

Standard error for K=0,079

Weighted K=0,762 good agreement

	Op. 2						
Op. 1		Grade 1	Grade 2	Grade 3	Grade 4	Grade 5	TOTAL
	Grade 1	4	4	0	0	0	8
	Grade 2	0	17	1	0	0	18
	Grade 3	0	0	3	2	0	5
	Grade 4	0	0	1	8	2	11
	Grade 5	0	0	0	3	15	18
	TOTAL	4	21	5	13	17	60

Table 16. Agreement between Operator 1 and Operator 2 concerning Score 2.

K=0,713 good agreement

Standard error for K=0,068

Weighted K=0,863 very good agreement

	Op. 1						
Op. 3		Grade 1	Grade 2	Grade 3	Grade 4	Grade 5	TOTAL
	Grade 1	8	8	0	0	0	16
	Grade 2	0	9	0	0	0	9
	Grade 3	0	1	3	4	0	8
	Grade 4	0	0	2	5	5	12
	Grade 5	0	0	0	2	13	15
	TOTAL	8	18	5	11	18	60

Table 17. Agreement between Operator 3 and Operator 1 concerning Score 2.

K=0,54 moderate agreement

Standard error for K=0,074

Weighted K=0,786 good agreement

	Op. 2						
Op. 3		Grade 1	Grade 2	Grade 3	Grade 4	Grade 5	TOTAL
	Grade 1	4	12	0	0	0	16
	Grade 2	0	8	1	0	0	9
	Grade 3	0	1	4	3	0	8
	Grade 4	0	0	0	10	2	12
	Grade 5	0	0	0	0	15	15
	TOTAL	4	21	5	13	17	60

Table 18. Agreement between Operator 3 and Operator 2 concerning Score 2.

K=0,606 good agreement

Standard error for K=0,070

Weighted K=0,811 very good agreement

In order to obtain the degree of agreement between the operators and the objective score the hardness values obtained using the integrated software (Esaote MyLab 70) have been traced to the score systems (Score 1 and 2). We refer to these values as “objective score”.

	MyLab					
Operator 1		Grade 1	Grade 2	Grade 3	Grade 4	TOTAL
	Grade 1	8	7	1	0	16
	Grade 2	0	9	2	0	11
	Grade 3	0	1	8	0	9
	Grade 4	0	0	7	17	24
	TOTAL	8	17	18	17	60

Table 19. Agreement between Objective score (MyLab) and Operator 1 concerning Score 1.

K=0,602 good agreement

Standard error for K=0,074

Weighted K=0,752 good agreement

	MyLab					
Operator 2		Grade 1	Grade 2	Grade 3	Grade 4	TOTAL
	Grade 1	8	8	1	0	17
	Grade 2	0	8	3	0	11
	Grade 3	0	1	6	0	7
	Grade 4	0	0	8	17	25
	TOTAL	8	17	18	17	60

Table 20. Agreement between Objective score (MyLab) and Operator 2 concerning Score 1.

K=0,538 moderate agreement

Standard error for K=0,075

Weighted K=0,718 good agreement

	MyLab					
Operator 3		Grade 1	Grade 2	Grade 3	Grade 4	TOTAL
	Grade 1	6	6	0	0	12
	Grade 2	2	11	2	0	15
	Grade 3	0	0	11	2	13
	Grade 4	0	0	5	15	20
	TOTAL	8	17	18	17	60

Table 21. Agreement between Objective score (MyLab) and Operator 3 concerning Score 1.

K=0,619 good agreement

Standard error for K=0,077

Weighted K=0,764 good agreement

	MyLab						
Op. 1		Grade 1	Grade 2	Grade 3	Grade 4	Grade 5	TOTAL
	Grade 1	0	8	0	0	0	8
	Grade 2	1	14	3	0	0	18
	Grade 3	0	0	3	2	0	5
	Grade 4	0	0	2	8	1	11
	Grade 5	0	0	0	8	10	18
	TOTAL	1	22	8	18	11	60

Table 22. Agreement between Objective score (MyLab) and Operator 1 concerning Score 2.

K=0,457 moderate agreement

Standard error for K=0,076

Weighted K=0,723 good agreement

	MyLab						
Op. 2		Grade 1	Grade 2	Grade 3	Grade 4	Grade 5	TOTAL
	Grade 1	0	3	0	0	0	3
	Grade 2	2	18	2	0	0	22
	Grade 3	0	0	4	1	0	5
	Grade 4	0	0	2	11	0	13
	Grade 5	0	0	0	6	11	17
	TOTAL	2	21	8	18	11	60

Table 22. Agreement between Objective score (MyLab) and Operator 2 concerning Score 2.

K=0,641 good agreement

Standard error for K=0,073

Weighted K=0,813 very good agreement

	MyLab						
Op. 3		Grade 1	Grade 2	Grade 3	Grade 4	Grade 5	TOTAL
	Grade 1	2	14	0	0	0	16
	Grade 2	0	6	3	0	0	9
	Grade 3	0	2	4	2	0	8
	Grade 4	0	0	0	10	0	10
	Grade 5	0	0	0	6	11	17
	TOTAL	2	22	7	18	11	60

Table 23. Agreement between Objective score (MyLab) and Operator 3 concerning Score 2.

K=0,450 moderate agreement

Standard error for K=0,072

Weighted K=0,723 good agreement

	Weighted K Score 1	Weighted K Score 2
Operator 1 VS Operator 2	0,891	0,863
Operator 2 VS Operator 3	0,762	0,811
Operator 1 VS Operator 3	0,849	0,786
Medium Value weighted K	0,834	0,820

Table 24. Agreement between operators concerning Score 1 and 2.

	Weighted K Score 1	Weighted K Score 2
Operator 1 VS Objective score	0,752	0,723
Operator 2 VS Objective score	0,718	0,813
Operator 3 VS Objective score	0,764	0,723
Medium Value weighted K	0,745	0,753

Table 25. Agreement between operators and objective scores for Score 1 and 2.

The Student's t test was used for assessing the existence of a statistical significant difference between benign and malignant lesions using the hardness values (HRD%). In order to apply this test to our sample we had to test the hypothesis of normality of the distribution of the two populations

(benign and malignant lesions). Then we confirmed the hypothesis that the two populations enjoyed the property of homoskedasticity.

	Malignant	Benign
Number	37	23
Medium value	69,47	36,76
Standard deviations	24,92	23,97
Min. Value	11,15	9,15
Max. Value	100	99,6
P	0,000005309	

Table 26. Data and P value of the Student's t test applied to benign and malignant lesion populations.

Finally we used the Pearson's Chi-square test for nominal variables to assess whether there was no statistically significant difference between benign and malignant lesions also using the objective score.

GRADE	Malignant	Benign	Total
1	2	6	8
2	6	11	17
3	13	5	18
4	16	1	17
Total	37	23	60
P value	0,000445		

Table 27. Pearson Chi square test for Score 1

GRADE	Malignant	Benign	Total
1	0	1	1
2	6	16	22
3	7	0	7
4	14	5	19
5	10	1	11
Total	37	23	0
P value	0,000191		

Table 28. Pearson Chi square test for Score 2

7.4 Discussion

Our sample consisted of 23 benign and 37 malignant lesions; corresponding to 38% of benignity 62% of malignancy. The overrepresented benign lesion was lipoma (11 cases out of 23 total), followed by phlogosis, follicular benign lesion, panniculitis, sebaceous cyst, keratin cysts and umbilical hernia. Concerning malignant lesions the overrepresented lesion was mast cell tumors (30 out of 37 total) followed by mucocutaneous lymphoma, sarcoma and VTT. This result is in agreement with the literature considering that mast cell tumors represent the most common cutaneous tumor in dogs (accounting for 16% to 21% of cutaneous tumors) (Thamm, 2007) . It is important to emphasize as the prevalence of mast cell tumor in the clinical practice is not so high and as the high proportion of this diagnosis in our sample is related to the high incidence of this cancer in our cases due to the high number of tumor staging requests coming from the section of oncology in our hospital. Similarly, the distribution of the other lesions in our sample probably does not express the real epidemiology for our particular reality. The result obtained in the Student's t test and Pearson's chi square test allow us to say that there is a statistically significant difference between benign and malignant lesions evaluated by HV and score system respectively ($p < 0,05$). We observe that malignant lesions tend to have a lower deformability (higher percentage of hardness) while the benign lesions tend to be more deformable (lower percentage of hardness). This has already been shown and discussed in human medicine, for example in the study on prostate cancer (Zhang, 2014) rather than on the stiffness of malignant thyroid nodules (Monpeysen, 2013). This stiffness increasing can be explained considering the typical greater cells density of malignant tumors that can lead to an higher concentration of collagen (in mesenchymal tumors); or considering the presence of a

connective capsule which prevents the ultrasounds interactions. (Giurgiu, 2011; Pallwein, 2008). Arguing the distributions of the diagnosis in the various categories grades and scores we can see different information outlined as follows: most of lipomas (90%) are distributed between the grade 1 and 2 of both scoring systems and they are not present in the high grades; phlogosis, sebaceous and keratin cysts were classified as hard lesions (3 phlogosis out of 4 presented an HV of 78% and they were classified as grade 3-4 in score 1 while 4-5 in score 2 - the two cysts presented an HV of 69% and they were classified in grade 3 of score 1 and grade 4 of score 2). The hardness found in these lesions can be explained considering the incompressibility of fluids. The amount of fluid in inflammatory lesions can be a consequence of active hyperemia as the biological nature of cyst can lead to an amount of serous fluids in cystic lesions. The amount of fluid in these lesions can be represented by hard areas. The large number of mast cell tumors belong to grade 4-5 of score 2 (64% of mast cell tumors) and to grade 3-4 in score 1 (80%). However mast cell tumor have been classified in other categories. The inability of classify mast cell tumor in the same grade in score system depend to its biological behavior. For example, the inflammation degree of the tumor at that time of the elastosonographic examination could determine active hyperemia and then determine change of deformability of tissue. Similarly tumors containing necrotic areas could be more compressible. The 3 benign neoplasms of follicular origin and 2 cases of panniculitis remain within the grade 2 of both score (resulting hard for less than 40% of their section in score 2 and less than 50% in score 1). Finally lymphomas and sarcomas fall into the highest categories of scores indicative of greater hardness for 67%. However the small number of our sample and the lesions distribution it is not possible to identify an accurate "cut-off value" that allows to clearly differentiate malignant lesions from benign lesions. This may also depend on

the type of lesions that are taken into consideration. In fact, in this study we have deliberately inserted both lipomas as well as cystic lesions in order to evaluate their elastosonographic properties. In clinical practice, however, a cystic lesion can be easily distinguishable from other types of lesions and notoriously it does not provide any difficulty in characterization as benign lesions during a B-mode ultrasonographic examination. Is it possible therefore that in future studies a score cut-off value will be achieved for distinguishing malignant from benign lesions, by excluding that lesions that present a cystic appearance. Considering our results (Table 27) we can note that in score 1 a large number of benign and malignant lesions are classified in grade 1, 2 and 3. However in grade 4 there are 16 malignant lesions and just one benign lesion. The benign lesion was diagnosed as phlogosis. We can therefore conclude that if a nodule on the skin falls into the category 4 has a high probability that it can be identified as a malignant lesion. Observing the Table 28 we can see that, even in score system 2, there is a prevalence of benign lesions in the categories 1 and 2 while malignant lesions are overrepresented in categories 3 and 4. However the sample size and the particular distribution of the diagnosis does not allow us to speculate on any possibilities to define a cut-off value. Despite this we can see that the majority of malignant lesions evaluated is classified in categories 4 and 5. Considering the inter-observer agreement we can see that among all three operators there is a very good correlation in score evaluation. This means that different operators can be able to classify in a comparable way the cutaneous nodular lesions using a subjective qualitative score system using elastosonography. From the average values calculated for the weighed K, we can see that there is a better agreement among operators than between observer and the objective score. This aspect can reasonably depend on the fact that the human eye can perceive a limited change in colors and can estimate the distribution of a

small percentage of hard areas than a software. In fact there have been several cases in which the objective score presented a value with a minimum difference from the operators classification; but this difference was enough to determine a classification in another grade. Small variations of hardness can be perceived by a calculation software but can escape from the visual evaluation. However despite the variability between objective score and score evaluated by the operators did not observe wide differences between scores. Even if the results of our work are promising and statistically significant, our study shows some limitations. First of all we would like to reiterate that the small and limited number of cases may not fully represent the real distribution of similar lesions in dogs. The skin nodules assessed had a different anatomical location (i.e. back, chest, neck, hock, hip) that may have changed in some way their elastic response. We know that a lesion placed next to a hard structure (for example in the case of lesion of a limb) can be deformed in a greater extent than a lesion located next to a soft tissue (for example in the case of lesion on the back). We also emphasize that in our sample there are many cytological diagnosis that, though supported by many positive follow up, should be replaced by a more accurate histological diagnosis. Definitely more studies are needed to evaluate the clinical applicability of this technique on canine skin lesions; either by selecting more subjects and more homogeneous regarding diagnosis. Later it would be useful to consider other score systems that can allow a better distinguishability between lesions. The results obtained in this study are encouraging about the possibility of applying the elastosonography the nodular lesions of the skin. We have seen that this technique is able to differentiate benign and malignant lesions due to the change of elasticity of the tissues involved by malignant pathological processes. When an lesion is assigned to a high elastosonographic score we can consider it with an high probability as a

malignant lesion. However, the use of these two scores did not provide an accurate cut-off value in differentiating benign from malignant lesions in our sample. Anyway the very good agreement between operators and the good agreement between operators and objective score demonstrate the feasibility of this technique.

CHAPTER 8

CONCLUSIONS

8. Conclusions

In conclusion the Real Time Elastosonography is an executable, reproducible and repeatable ultrasonographic technique. With our studies, we ascertained that although the technique requires a few minutes to be performed, a certain level of training is needed before obtaining diagnostic and technically correct images. From the clinical point of view we can say that the Real Time Elastography represents a promising and potentially useful technique for the study of focal splenic lesions in dogs and potentially also for their ultrasonographic monitoring. Concerning canine subcutaneous lesions it resulted helpful in distinguishing benign from malignant lesions but nevertheless the clinical utility in this area remains limited. Contrary to what has been observed by others, in our study, Elastography resulted useless in the differentiation of mammary tumors in dogs. Further studies are needed to assess the applicability of this technique on other tissues such as lymph-nodes or thyroid.

CHAPTER 9

REFERENCES

9. References

1. Alam F, Naito K, Horiguchi J et al. Accuracy of sonographic elastography in the differential diagnosis of enlarged cervical lymph nodes: comparison with conventional B-mode sonography. *Am J Roentgenol*. 2008;191:601-610.
2. Alder D, Bass D, Sporri M et al. Does real time elastography aid in differentiating canine splenic nodules. *Schweizer Archiv* 2013;491-496.
3. Asteria C, Giovanardi A, Pizzocaro et al. Us-elastography in the differential diagnosis of benign and malignant thyroid nodules: a meta-analysis. *Thyroid* 2008;18:523-531.
4. Arda K, Ciledag N, Aktas E et al. Quantitative assessment of normal soft tissue elasticity using shear-wave ultrasound elastography. *Am J Roentgenol* 2011;197.
5. Bamber J, Cosgrove D, Dietrich CF et al. EFSUMB Guidelines and recommendations on the clinical use of ultrasound elastography. Part 1: basic principles and technology. *Ultraschall Med* 2013;34(3):169-184.
6. Barr RG. Real-time ultrasound elasticity of the breast: initial clinical results. *Ultrasound Q* 2010;26(2):61-66.
7. Barr RG, Lackey AE. The utility of the “bull’s eye” artifact on breast elasticity imaging in reducing breast lesion biopsy rate. *Ultrasound Q* 2011;27(3):151-155.
8. Barr R. Sonographic breast elastography: a primer. *J Ultrasound Med* 2012;31:77-783.
9. Barr R, Nakashima K, Amy D et al. WFUMB Guidelines and recommendations for clinical use of ultrasound elastography: part 2: breast. *Ultrasound Med Biol* 2015;41:1148-1160.
10. Bathia KS, Cho CC, Yuen YH et al. Real-time qualitative ultrasound elastography of cervical lymph nodes in routine clinical practice:

interobserver agreement and correlation with malignancy. *Ultrasound Med Biol* 2010;36:1990-1997.

11. Chalita MC, Matera JM, Alves MT et al. Nonaspiration fine needle cytology and its histologic correlation in canine skin and soft tissue tumors. *Annal Quant Cytol Histol* 2001;23:395–399.
12. Christensen NI, Canfield PJ, Martin PA et al. Cytopathological and histopathological diagnosis of canine splenic disorders. *Aust Vet J* 2009;87(5);175-181.
13. Ciurea AI, Dumitriu D, Ciortea C et al. Artifacts and pitfalls in breast elastoultrasonography: a pictorial essay. *Medical Ultrason* 2008; 10:93-98.
14. Cohen M, Bohling MW, Wright JC et al. Evaluation of sensitivity and specificity of cytologic examination: 269 cases (1999–2000). *J Am Vet Med Assoc* 2003;222:964–967.
15. Cole PA. Association of canine splenic haemangiosarcomas and hematoma with nodular lymphoid hyperplasia or siderotic nodules. *J Vet Diagn Investig* 2012;24(4);759-762.
16. Cosgrove D, Piscaglia F, Bamber J et al. EFSUMB Guidelines and recommendations on the clinical use of ultrasound elastography. Part 2: clinical applications. *Ultraschall Med* 2013; 34(3):238-253.
17. Dudea SM, Giurgiu CR, Dumitriu D et al. Value of ultrasound elastography in the diagnosis and management of prostate carcinoma. *Medical Ultrason* 2011;13:45-53.
18. Dudea SM, Botar-Jid C, Dumitriu D et al. Differentiating benign from malignant superficial lymph nodes with sonoelastography. *Medical Ultrason* 2013;15:132-139.
19. Feliciano MAR, Vicente WRR, Silva MAM. Conventional and Doppler ultrasound for the differentiation of benign and malignant canine mammary tumours. *J Small Anim Pract* 2012;53:332-337.

20. Feliciano MAR, Maronezi MC, Pavan L et al. ARFI elastography as a complementary diagnostic method for mammary neoplasia in female dogs-preliminary results. *J Small Anim Pract* 2014;55:504-508.
21. Ghisleni G, Roccabianca P, Ceruti R et al. Correlation between fine-needle aspiration cytology and histopathology in the evaluation of cutaneous and subcutaneous masses from dogs and cats. *Vet Clin Pathol* 2006;35(1):24-30.
22. Giurgiu CR, Manea C, Crisan N et al. Real-time sonoelastography in the diagnosis of prostate cancer. *Med Ultrason* 2011;13(1):5-9.
23. Glinska-Suchocka K, Jankowski M, Kubiak K et al. Application of shear wave elastography in the diagnosis of mammary gland neoplasm in dogs. *Pol J Vet Sci* 2013; 16(3):477-482.
24. Goddi A, Bonardi M, Alessi S. Breast elastography: A literature review. *J Ultrasound* 2012;15:192-19.
25. Greenleaf JF, Fatemi M, Insana M. Selected methods for imaging elastic properties of biological tissues. *Ann Rev Biomed Eng* 2003;5: 57-78.
26. Hall TJ, Zhu Y, Spalding CS. In vivo real-time freehand palpation imaging. *Ultrasound Med Biol* 2003;29(3):427-435.
27. Hayes G, Ladlow J. Investigation and management of splenic disease in dogs. *Practice* 2012;34(5);250-259.
28. Hirooka M, Ochi H, Koizumi Y et al. Splenic elasticity measured with real-time tissue elastography is a marker of portal hypertension. *Radiology* 2011;261(3):960-968.
29. Holdsworth A, Bradley K, Birch A et al. Elastography of the normal canine liver, spleen and kidneys. *Vet Radiol Ultrasound* 2014;55(6): 620-627.
30. Houle TT, Stump DA. Statistical significance versus clinical significance. *Semin Cardiothorac Vas Anesth* 2008;12:5-6.

31. Ishibashi N, Yamagata K, Sasaki H et al. Real-time tissue elastography for the diagnosis of lymph node metastasis in oral squamous cell carcinoma. *Ultrasound Med Biol* 2012;38(3):389-395.
32. Itoh A, Ueno E, Tohno et al. Breast disease: clinical application of us elastography for diagnosis. *Radiology* 2006;239:341-350.
33. Ivancic M, Long F, Seiler GS. Contrast harmonic ultrasonography of splenic masses and associated liver nodules in dogs. *J Am Vet Med Assoc* 2009;234:88–9.
34. Jeon S, Lee G, Lee SK et al. Ultrasonographic elastography of the liver, spleen, kidneys and prostate in clinically normal beagle dogs. *Vet Radiol Ultrasound* 2015;00:1-7.
35. Juarez AR, Morgaz J, Camacho A et al. Liver stiffness using Transient Elastography is applicable to canines for hepatic disease models. *PLoS ONE* 2012;7(7):e41557.
36. Jun-Young K, Nam-Soon L, Mittyun C et al. Correlation of ultrasonographic findings and cytologic or histopathologic diagnoses of splenic lesions in dogs: 124 cases. *J Vet Clin* 2012;29:134-140.
37. Lana SE, Rutteman GR, Withrow SJ, Tumors of the mammary gland. In Withrow SJ, Vail DM, editors, Withrow and Macewen's *Small animal clinical oncology*. Fourth edition; 2007; 619-636.
38. Lee G, Jeon S, Lee SK et al. Strain elastography using dobutamine-induced carotid artery pulsation in canine thyroid gland. *Vet Radiol Ultrasound* 2015;56(5): 549-553.
39. Lustgarten M, Redding WR, Bens R et al. Elastographic characteristics of the metacarpal tendons in horses without clinical evidence of tendon injury. *Vet Radiol Ultrasound* 2014;55(1):92-101.
40. Lyshchick A, Higashi T, Asato R et al. Cervical lymph node metastasis : diagnosis at sonoelastography-initial experience. *Radiology* 2007;243:258-267.

41. Monpeyssen H, Tramalloni J, Poiree S et al. Elastography of the thyroid. *Diagnostic and Interventional Imaging* 2013;94:535-544.
42. Nazarian LN. Can sonoelastography enable reliable differentiation between benign and metastatic cervical lymph nodes?. *Radiology* 2007;243:1.
43. Ohlerth S, Dennler M, Ruefli E, et al. Contrast harmonic imaging characterization of canine splenic lesions. *J Vet Intern Med* 2008;22: 1095–1102.
44. Ophir J, Alam SK, Garra B et al. Elastography: ultrasonic estimation and imaging of the elastic properties of tissues. *Proc In St Mech Eng H* 1999;213:203-233.
45. Pallwein L, Aigner F, Faschingbauer R et al. Prostate cancer diagnosis: value of real-time elastography. *Abdom Imaging* 2008;33(6):729-35.
46. Pallwein L, Mitterberger M, Pinggera G et al. Sonoelastography of the prostate: Comparison with systematic biopsy findings in 492 patients. *Eur J Radiol* 2008;65(2):304-10.
47. Queiroga F, Lopes C. Canine mammary tumors-new perspectives. *Annals of Congress of Veterinary Science, Oeiras, Brazil* 2002; 183-190.
48. Rossi F, Leone VF, Vignoli M et al. Use of contrast enhanced ultrasound for characterization of focal splenic lesions. *Vet Radiol Ultrasound* 2008;49(2);154-164.
49. Roush JK. The potential tyranny of statistical power. *Vet Comp Orthop Traumatol* 2015; 28(3):225.
50. Sarvazyan A, Hall TJ, Urban MW et al. An overview of elastography: an emerging branch of medical imaging. *Curr Med Imaging* 2011;7:255-282.
51. Sharpley JL, Marolf AJ, Reichle JK et al. Color and power Doppler ultrasonography for characterization of splenic masses in dogs. *Vet Radiol Ultrasound* 2012;55(5):586-590.

52. Shiina T. Ultrasound elastography: Development of novel technologies and standardization. *Jpn J Appl Phys* 2014;53:07KA02.
53. Simenov RS. The accuracy of fine-needle aspiration cytology in the diagnosis of canine skin and subcutaneous masses. *Comp Clin Pathol* 2012;21(2):143-7.
54. Taeymans O, Penninck D. Contrast enhanced sonographic assessment of feeding vessels as a discriminator between malignant vs. benign for a splenic lesions. *Vet Radiol Ultrasound* 2011;52(4):457-461.
55. Thamm Dh, Vail DM. Mast cell tumors. In Withrow SJ, Vail DM, editors, Withrow and Macewen's *Small animal clinical oncology*. Fourth edition; 2007; 402.
56. Teng D, Wang H, Lin Y et al. Value of ultrasound elastography in assessment of enlarged cervical lymphnodes. *Asian Pac J Cancer Prev* 2012;13:2081-2085.
57. Wang H, Brylka D, Sun L et al. Comparison of strain ratio with elastography score system in differentiating malignant from benign thyroid nodules. *Clin Imaging* 2013;37:50-55.
58. Watson AT, Penninck D, Knoll JS et al. Safety and correlation of test results of combined ultrasound guided fine-needle aspiration and needle core biopsy of the canine spleen. *Vet Radiol Ultrasound* 2011;52(3): 317-322.
59. Wells PN, Liang HD. Medical ultrasound: imaging of soft tissue strain and elasticity. *J R Soc Interface* 2011;8:1521-1549.
60. White J, Gay J, Farnsworth R et al. Ultrasound elastography of the liver, spleen and kidneys in clinically normal cats. *Vet Radiol Ultrasound* 2013;00:1-7.
61. Wojcinski S, Dupont J, Schmidt W et al. Real-time ultrasound elastography in 180 axillary lymph nodes: elasticity distribution in

healthy lymph nodes and prediction of breast cancer metastasis. *BMC Med Imaging* 2012;12:35.

62. Zhang B, Ma X, Zhan W, et al. Real-time elastography in the diagnosis of patients suspected of having prostate cancer: a meta-analysis. *Ultrasound Med Biol* 2014; 40(7):1400-7.
63. Zhou JQ, Zhou C, Zhan WW et al. Elastography ultrasound for breast lesions: fat-to-lesion strain ratio vs gland-to-lesion strain ratio. *Eur Radiol* 2014;24:3171-3177.